FM Proton Irradiation Tests High & Low Stress Modules II : Noise evolution, Curing frequency, Detector settings

PICC-KL-TN-023

Prepared by	P.Royer	
Approved by		
Authorised by		

Distribution List

Recipients	*Affiliation*	*Nr. of Copies*

Document Change Record

Issue	*Date*	*Description*
Draft 1	20/03/06	NEP plotted = median over all pixels
Draft 2	27/03/06	. Detectors covered by the FIR filter or not considered separately . Inclusion of the discussion on curing frequency & det. settings
Draft 3	31/03/06	Flux assumption corrected for LS data. All LS-NEP plots renewed
Draft 4	04/04/06	. Y-axis divided by 2 in all NEP plots (see section 4.1) . Discussion on NEPs (section 5.2) extended. . Section 6 revamped. . Conclusions updated.
Draft 5	10/04/06	Minor modifications

Table of Contents

1 Introduction

One high and one low stress modules of PACS spectrometer detectors were tested under proton irradiation at the cyclotron of Louvain-la-Neuve in Belgium (UCL). This happened under representative FIR flux, on 7 & 8 April 2005 for the high stress (HS) module and 4 & 5 October 2005 for the low stress (LS). The aim of this document is to report on the evolution of the noise along the time and wrt the various detector setting which were tested. This will be done through a 'chopping exercise' similar to that presented in RD04, with the addition that we will this time take into account the effect of glitches and we will not take into account those ramps obviously affected by a glitch.

2 Reference Documents

RD01 PACS-ME-TP-009 version 1.2 Test plan and procedure for investigation of glitch event rate during proton irradiation (1st test phase)

RD02 PACS-ME-TP-009 version 2.2 Test plan and procedure for investigation of glitch event rate during proton irradiation (2nd test phase)

RD03 PACS-ME-TP-009 version 3.1 Test plan and procedure for investigation of glitch event rate during proton irradiation (3rd test phase)

RD04 PICC-KL-TN-013 CQM Proton irradiation test analysis. Noise evolution.

RD05 PICC-KL-TN-018 Spectral line scan simulations on PACS HS modules under proton irradiation

RD06 PICC-KL-TN-022 FM Proton Irradiation Tests : High & Low stress modules. I. Glitch effects & curing.

RD07 PICC-KL-TN-011 CQM Proton irradiation test analysis

3 Data

A description of the test setup, test procedure and resulting data for both FM test campains can be found in RD01, RD02 & RD03. It suffices here to say that there were 3 test campains, one for a QM HS module, one for a FM HS module and one for a FM LS module. Each time. two proton fluxes were used. Typically a low flux, being ~ 10 p/cm^2/s, and a higher flux, simulating a solar flare, being ~400 p/cm^2/s. The modules were operated in a nominal way during the tests, under representative FIR background. In the 2 most recent test campains, a FIR filter representative of that in the PACS instrument was also placed in front of 'lower' 8 detectors (in terms of numerotation). Hence, detectors 1 to 8 received a smaller flux than detectors 9 to 16.

We will here refer to the data files by abbreviated names refering either to HS or LS data, and starting with the letter N, L and H for No, Low and High proton flux respectively, and following the same numerotation than RD01 to RD03. So, for instance, T25b80d10t025c04n256_N_33.dat of RD03 becomes HS_N33, or N33 if there is no ambiguity on which module we are talking about. The detector setup parameters can be obtained directly from the filename in RD01 to RD03.

An analysis of the QM test data similar to the one we aim at herein was presented in RD04. For the sake of comparison, we re-did this analysis with the modified code we used for the analysis of the FM data. The detailed list of files analysed for each of the 3 test campains is

- QM HS module : same set of files as in RD04 (see section 1 in RD07 & figure 1 below).
- FM HS module : same set of files as in RD05 (see figure 2 inthere)
- FM LS module : the chosen files cover 2 'growing phases' from cured detectors to high responsivity, as well as the full sequence of tests with various detector settings (bias from 80 to 200mV, ramp length from 1 to 1/16 second). The exact list is presented below for reference.

0 T25b120t025c14n256_#N_5.dat	51 T25b120t025c14n1024_#L_107.dat
1 T25b120t025c14n256_#N_15.dat	52 T25b120t025c14n1024_#L_108.dat
2 T25b120t025c14n256_#N_27.dat	53 T25b120t025c14n1024_#L_109.dat
3 T25b120t025c14n1024_#L_65.dat	54 T25b120t025c14n1024_#L_110.dat
4 T25b120t025c14n1024_#L_66.dat	55 T25b120t025c14n1024_#L_111.dat
5 T25b120t025c14n1024_#L_67.dat	56 T25b120t025c14n1024_#L_112.dat
6 T25b120t025c14n1024_#L_68.dat	57 T25b120t1c14n64_#L_113.dat
7 T25b120t025c14n1024_#L_69.dat	58 T25b120t05c14n128_#L_114.dat
8 T25b120t025c14n1024_#L_70.dat	59 T25b120t025c14n256_#L_115.dat
9 T25b120t025c14n1024_#L_71.dat	60 T25b120t0125c14n512_#L_116.dat
10 T25b120t025c14n1024_#L_72.dat	61 T25b120t00625c14n1024_#L_117.dat
11 T25b120t025c14n1024_#L_73.dat	62 T25b100t1c14n64_#L_118.dat
12 T25b120t025c14n1024_#L_74.dat	63 T25b100t05c14n128_#L_119.dat
13 T25b120t025c14n1024_#L_75.dat	64 T25b100t025c14n256_#L_120.dat
14 T25b120t025c14n1024_#L_76.dat	65 T25b100t0125c14n512_#L_121.dat
15 T25b120t025c14n1024_#L_77.dat	66 T25b100t00625c14n1024_#L_122.dat
16 T25b120t025c14n1024_#L_78.dat	67 T25b80t025c14n256_#N_9.dat
17 T25b120t025c14n1024_#H_1.dat	68 T25b80t025c14n256_#N_31.dat
18 T25b120t025c14n1024_#H_2.dat	69 T25b80t1c14n64_#L_123.dat
19 T25b120t025c14n1024_#H_3.dat	70 T25b80t05c14n128_#L_124.dat
20 T25b120t025c14n1024_#H_4.dat	71 T25b80t025c14n256_#L_125.dat
21 T25b120t025c14n1024_#H_5.dat	72 T25b80t0125c14n512_#L_126.dat
22 T25b120t025c14n1024_#H_6.dat	73 T25b80t00625c14n1024_#L_127.dat
23 T25b120t025c14n1024_#L_79.dat	74 T25b140t1c14n64_#L_128.dat
24 T25b120t025c14n1024_#L_80.dat	75 T25b140t05c14n128_#L_129.dat
25 T25b120t025c14n1024_#L_81.dat	76 T25b140t025c14n256_#L_130.dat
26 T25b120t025c14n1024_#L_82.dat	77 T25b140t0125c14n512_#L_131.dat
27 T25b120t025c14n1024_#L_83.dat	78 T25b140t00625c14n1024_#L_132.dat
28 T25b120t025c14n1024fl4_#L_84.dat	79 T25b160t1c14n64_#L_133.dat
29 T25b120t025c14n1024_#L_85.dat	80 T25b160t05c14n128_#L_134.dat
30 T25b120t025c14n1024_#L_86.dat	81 T25b160t025c14n256_#L_135.dat
31 T25b120t025c14n1120fl05_#L_87.dat	82 T25b160t0125c14n512_#L_136.dat
32 T25b120t025c14n1024_#L_88.dat	83 T25b160t00625c14n1024_#L_137.dat
33 T25b120t025c14n1024_#L_89.dat	84 T25b180t1c14n64_#L_138.dat
34 T25b120t0125c14n2240fl05_#L_90.dat	85 T25b180t05c14n128_#L_139.dat
35 T25b120t00625c14n4480fl05_#L_91.dat	86 T25b180t025c14n256_#L_140.dat
36 T25b120t05c14n560fl05_#L_92.dat	87 T25b180t0125c14n512_#L_141.dat
37 T25b120t1c14n280fl05_#L_93.dat	88 T25b180t00625c14n1024_#L_142.dat
38 T25b120t025c14n1024_#L_94.dat	89 T25b60t1c14n64_#L_143.dat
39 T25b120t1c14n64_#L_95.dat	90 T25b60t05c14n128_#L_144.dat
40 T25b120t05c14n128_#L_96.dat	91 T25b60t025c14n256_#L_145.dat
41 T25b120t025c14n256_#L_97.dat	92 T25b60t0125c14n512_#L_146.dat
42 T25b120t0125c14n512_#L_98.dat	93 T25b60t00625c14n1024_#L_147.dat
43 T25b120t00625c14n1024_#L_99.dat	94 T25b200t1c14n64_#L_148.dat
44 T25b120t025c14n1024_#L_100.dat	95 T25b200t05c14n128_#L_149.dat
45 T25b120t025c14n1024_#L_101.dat	96 T25b200t025c14n256_#L_150.dat
46 T25b120t025c14n1024_#L_102.dat	97 T25b200t0125c14n512_#L_151.dat
47 T25b120t025c14n1024_#L_103.dat	98 T25b200t00625c14n1024_#L_152.dat
48 T25b120t025c14n1024_#L_104.dat	99 T25b200t025c14n256_#N_1.dat
49 T25b120t025c14n1024_#L_105.dat	100 T25b120t025c14n1024_#L_153.dat
50 T25b120t025c14n1024_#L_106.dat	

Table 1. Datafiles belonging to the FM LS run analysed hereafter, with their numerotation in the figures.

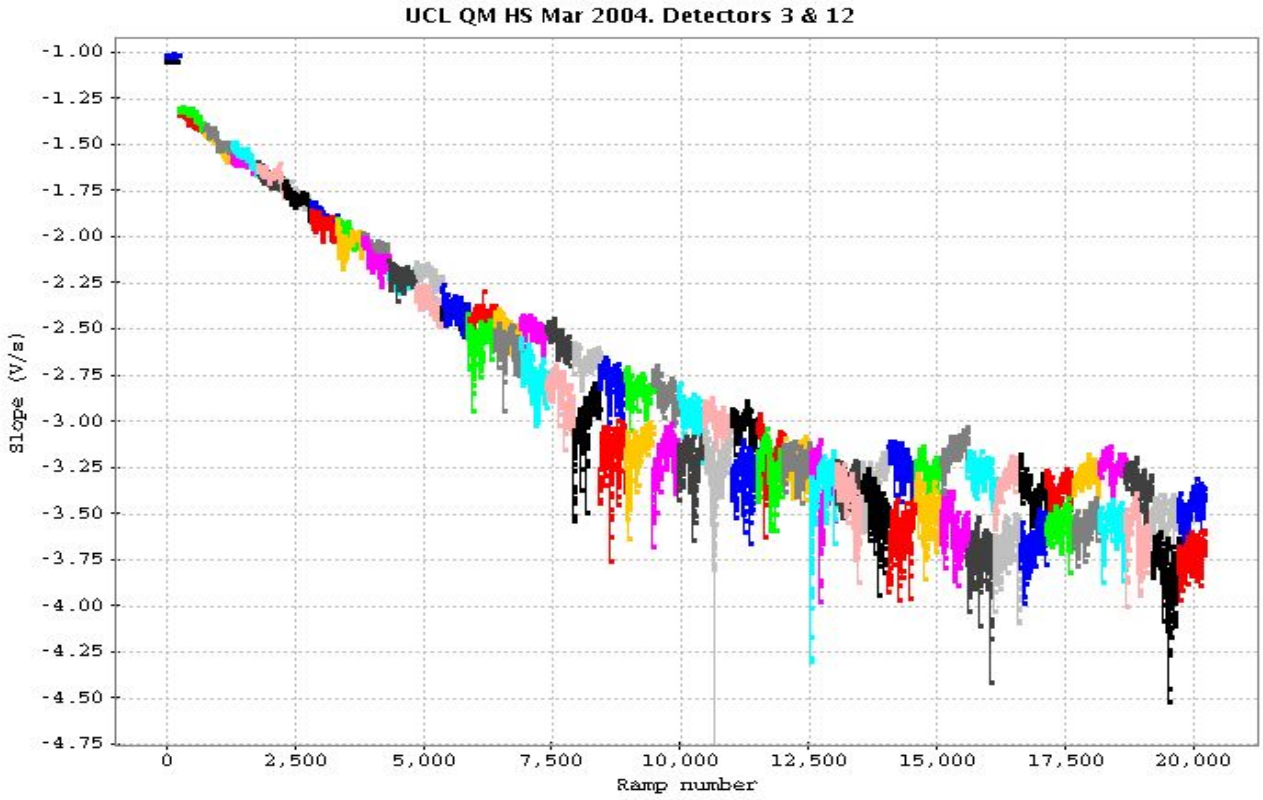

Figure 1 : slopes vs ramp number for the QM HS data analysed here (see also RD04 & RD07). The first data file is a pre-beam reference.

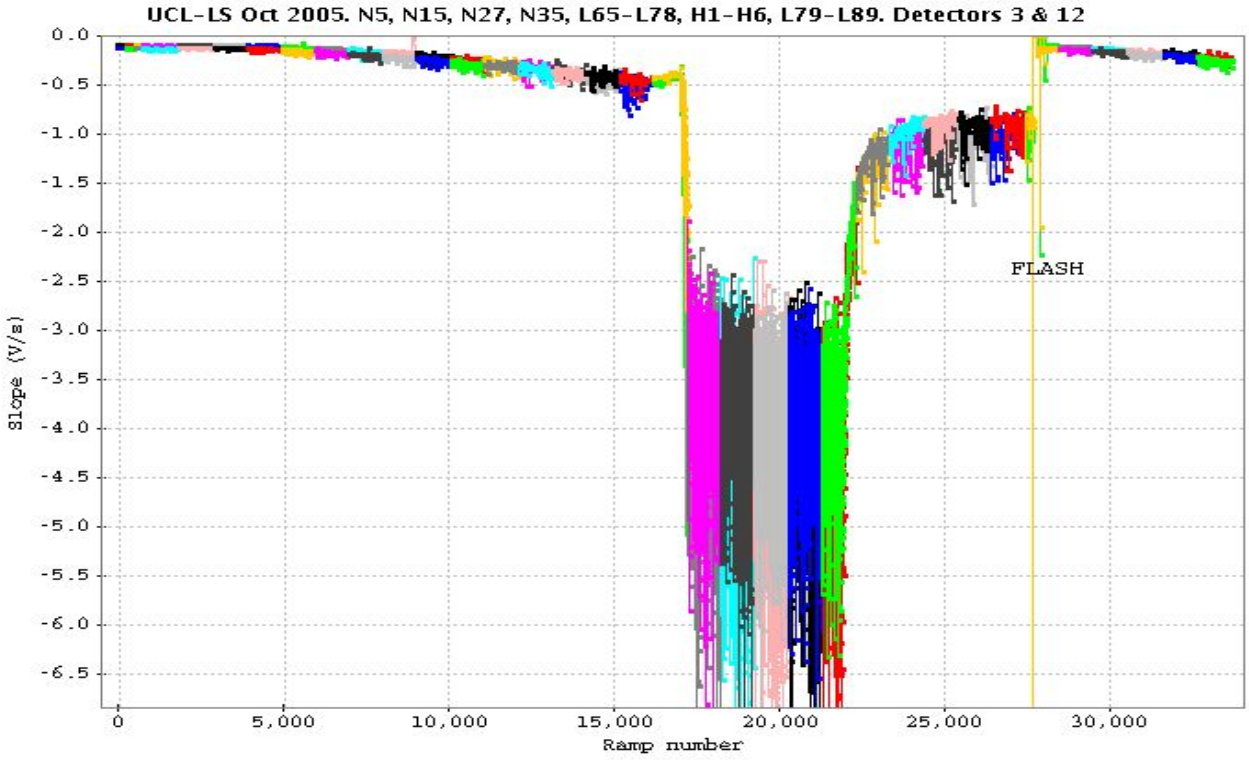

Figure1. UCL-FM Low Stress detector module data. Files L65 to L89 (see also RD06).

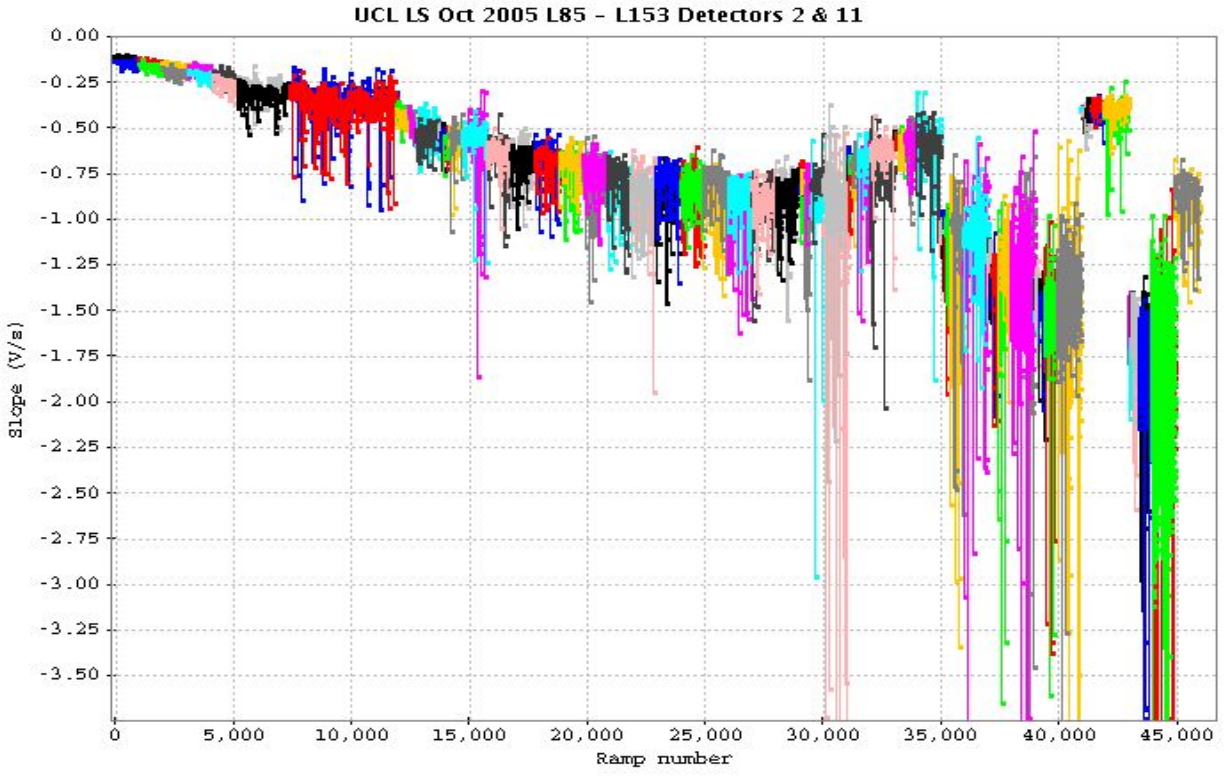

Figure 2 : UCL-FM Low Stress detector module data. Files L85 to L153. The plateau of high responsivity is reached towards L110 (ramp ~26000). The seemingly chaotic behaviour of the responsivity towards the end of the sequence comes from the variety of detector settings tested from file L113 on (= from ramp ~29000).

4 Methodology

4.1Virtual Chopping

The NEPs plotted hereafter were established in a 'simulated chopping exercise' absolutely similar to the procedure described in RD04. Nevertheless, **after the computation, the NEPs were divided by 2** for the plots*. Indeed, the NEPs computed through this simulated chopping exercise are a factor 2 higher than the “real” NEPs computed directly on the ramps (this was of course established on pre-beam data were it's possible to compute the NEP via both ways). The reason is twofold

- the normalisations factor is higher by sqrt(2) in the chopping exercise :
  - direct NEP computation : normalisation

    = sqrt (2 * nsamp/256)

    = sqrt(duration of 2 ramps) (see PACS-IM-PS-001)
  - chopped exercise : normalisation

    = sqrt (2 * choplen * 2 * nsamp/256) = sqrt(4 chopper plateaus)

    = sqrt (duration of 2 flux measures)

  The noise improvement obtained with longer chopper plateau is compensated by the sqrt(choplen), hence leaving exactly a sqrt(2) difference between both methods, whatever choplen.

- the fluxes computed in the chopping exercise result from a subtraction, which naturally increases the noise by sqrt(2).

4.2 Rejection of Responsivity Jumps

The exception to what was just said is that, in addition to the basic procedure of RD04, we tried to take the presence of glitches into account through their effects on the slopes/responsivity. This implies

1. detection of the responsivity glitches (either true and discrete evolution of the responsivity, like often happens for the HS detectors, or isolated high slope being an indirect effect of the underlying glitch, like often the case for LS detectors, see RD05).
2. rejection of the affected slopes. This was done in the most basic way : the ramps flagged as being affected by a responsivity jump (hereafter RJ) were simply ignored from further computation. To be precise, this means that we always considered chopper plateaus of the same lengths (say n), although the signal we kept from them was sometimes the average of n-k ramps, where k is the number of RJ flags set on the ramps of this chopper plateau. If any of 2 consecutive chopper plateaus was found to have all ramps flagged as RJ, then the 2 chopper plateaus were ignored.

The detection of the RJ was based on a q-test outlyer detection code. In just a few words

1. let's note 'sl' the slopes vs time signal
2. compute dsl = sl[i+1] – sl[i] and ds2 = sl[i+1] – sl[i-1]
3. chose a window size (units : ramps; e.g. width w = 16 or 32 ramps)
4. compute the q-test score of dsl & ds2 for a box of width 'w' sliding over the signal, i.e. q-score of the convolution of dsl & ds2 with a square box of width w.
5. At step 4, each slope gets w different q-scores for dsl & w others for ds2. Keep the maximum values for each ramp (one value for dsl, forming the q1 vector, one for ds2, forming the q2 vector).

* Note that this was **NOT** done in RD04, nor in RD05!

6. Threshold q1 & q2 with a procedure specifically tuned to the type of events present in our data (this implies 3 to 4 different threshold values, which, once established, are valid for all data. The product here is a boolean vector flagging those ramps suspected to suffer from a RJ.
7. In sl, replace the slopes flagged as RJ on step 6 by the average of their closest non-flagged slopes. Let's note this new signal sl2 (this step takes place only if n>1, see step 8)
8. Repeat steps 2 to 7 'n' times, each time merging the boolean vectors created at step 6.

This procedure, though not perfect, produces very valuable results. For the record, the parameters we finally kept for this analysis are

w = 16, n=1, thresholds = 5., 0.7, 0.7, 0.4

Figures 3 & 4 show examples of RJ flagged with various sets of parameters in the case of HS & LS data.

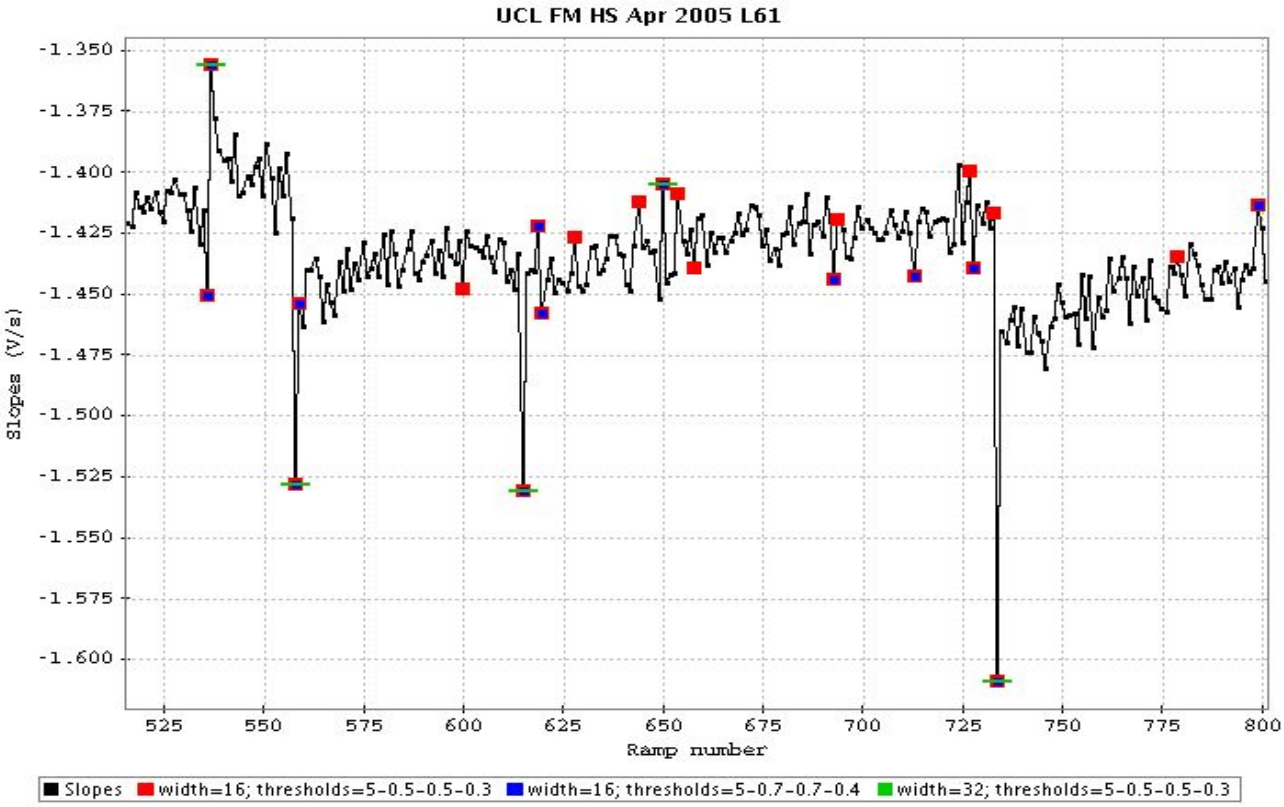

Figure 3 : RJ flagged on datafile FM HS L61. In HS data, most RJ exhibit a long term effect. Hence, ignoring the RJ itself is not sufficient to get rid of its effects.

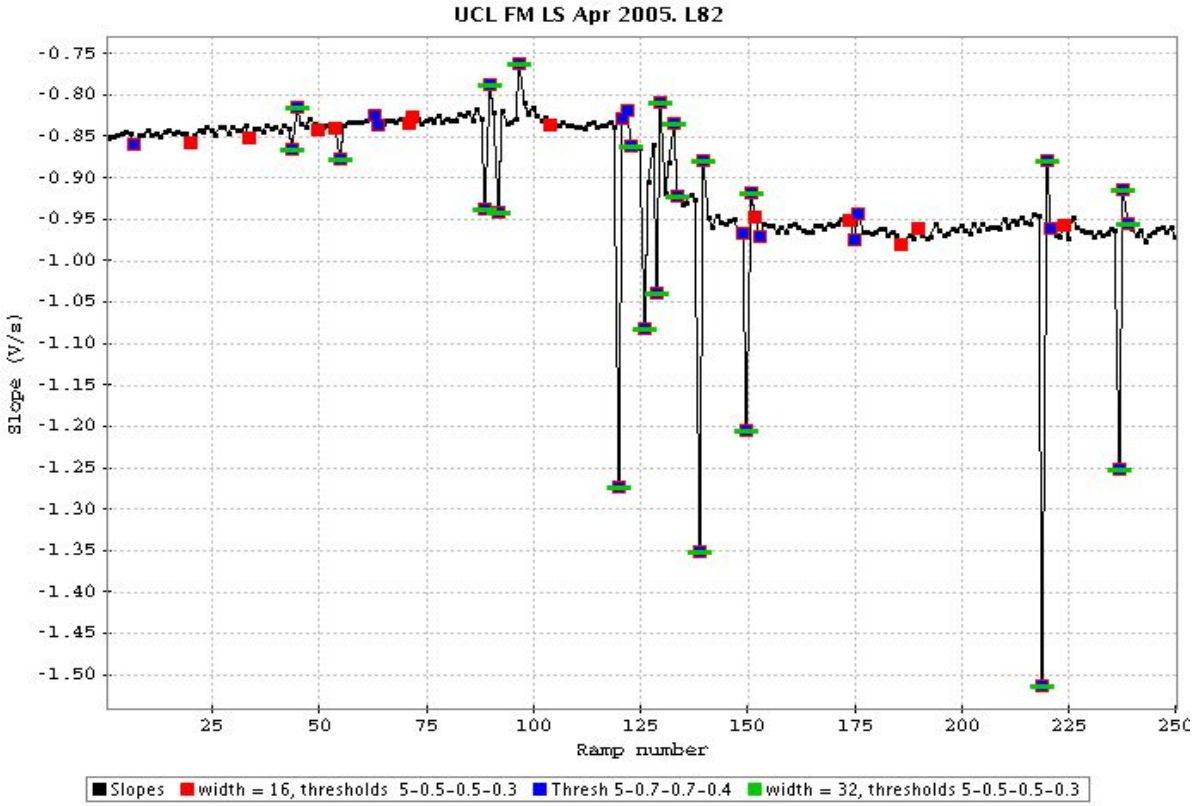

Figure 4 : RJ flagged on datafile FM LS L82. In LS data, most RJ exhibit no long term effect, but simply correspond to the direct effect of the glitch on the fitted slope. Hence ignoring the RJs solves most of the issues

5.Noise evolution & detector settings

5.1 First test run : QM HS

For the sake of comparison with previous results, we reproduced the results exposed in RD04. It is also a very nice way to introduce the effects of the RJ detection / deletion on the final result.

Figure 5 shows the results obtained for chopper plateaus of 1 and 4 ramps.

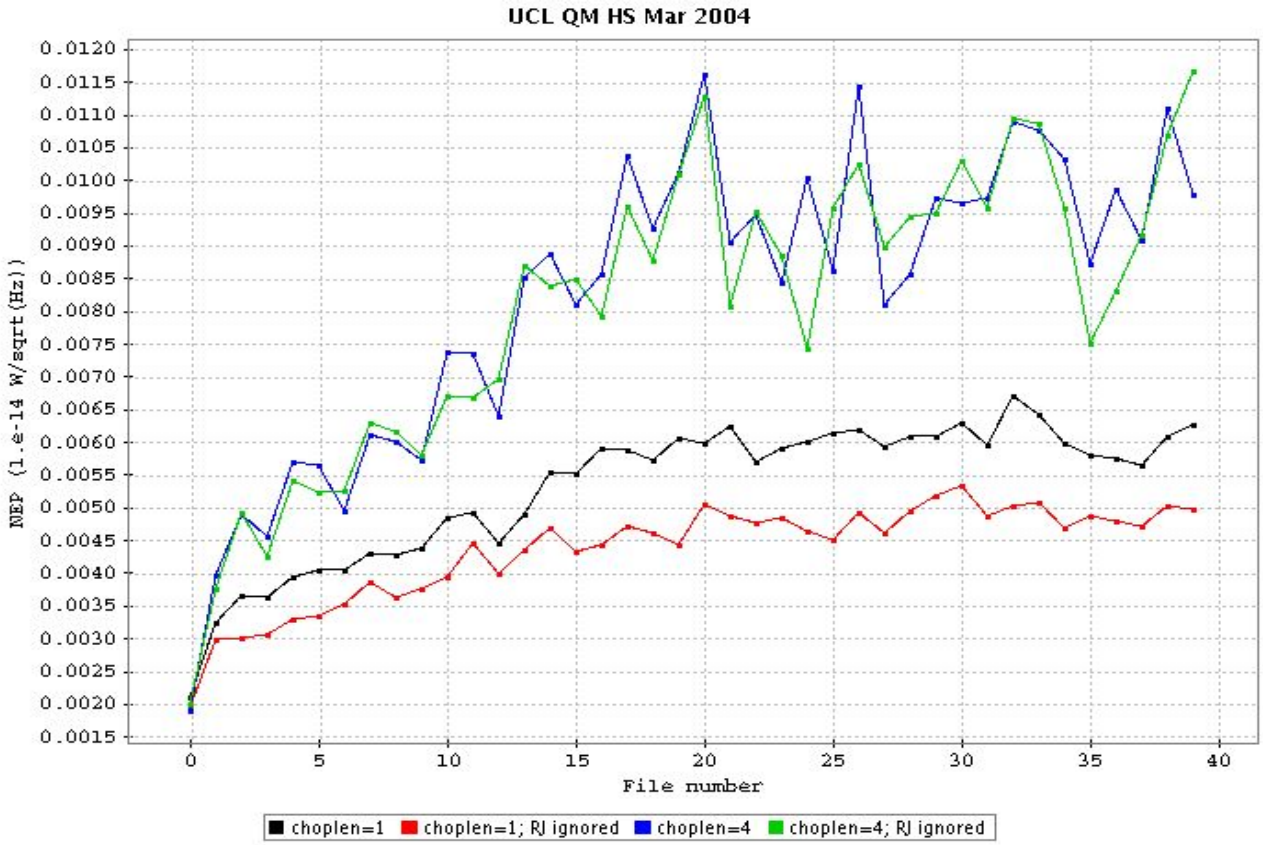

Figure 5. Evolution of NEP (median over all pixels) with time (hence, here, responsivity) for the QM HS data (the black and blue curves perfectly match their equivalents in RD04). The flux was supposed = 1.e-14W / pix. The bias, Cf & ramp duration were 70mV, 3pF & 0.3 second respectively.*

The main **conclusions** of this are that

- the noise is increasing with responsivity. The first file, being pre-irradiation, exhibits a much lower noise. Then, the noise is progressively increasing along with the responsivity (see figure 1).
- The noise is higher for longer chopper plateau.
- The rejection of RJ is efficient for a length of chopper plateau (hereafter choplen) of 1, but not at all for chopper plateaus of 4 ramps. The explanation of this can be found in figure 3, or e.g. figure 16 in RD06, and it's simple: in the signal of HS modules, glitches often produce long term effects on the responsivity, i.e. the responsivity is in a 'low state' before the glitch, and in a 'higher state' for all subsequent ramps. Hence, with any value of choplen > 1 (think 4), we cannot avoid the chopping process to combine ramps from both high and low responsivity states in a single flux measure. On the countrary, with choplen =1, we are sure that this never happens, hence strongly reducing the noise when taking out the RJs.

* Recalibrations indicated that the flux was actually twice as high! Hence all NEPs in this figure should be doubled!

5.2 Second test run : FM HS

Figure 6 to 8 show simular results as Figure 5, but this time for the FM HS module tests (second run in UCL-CRC, Apr 2005). In all these figures, the flux assumption were the following :

- "low detectors" (covered by the FIR filter) : 2. e-15W/pix
- "high detectors" (not covered by the FIR filter) : 5. e-15W/pix

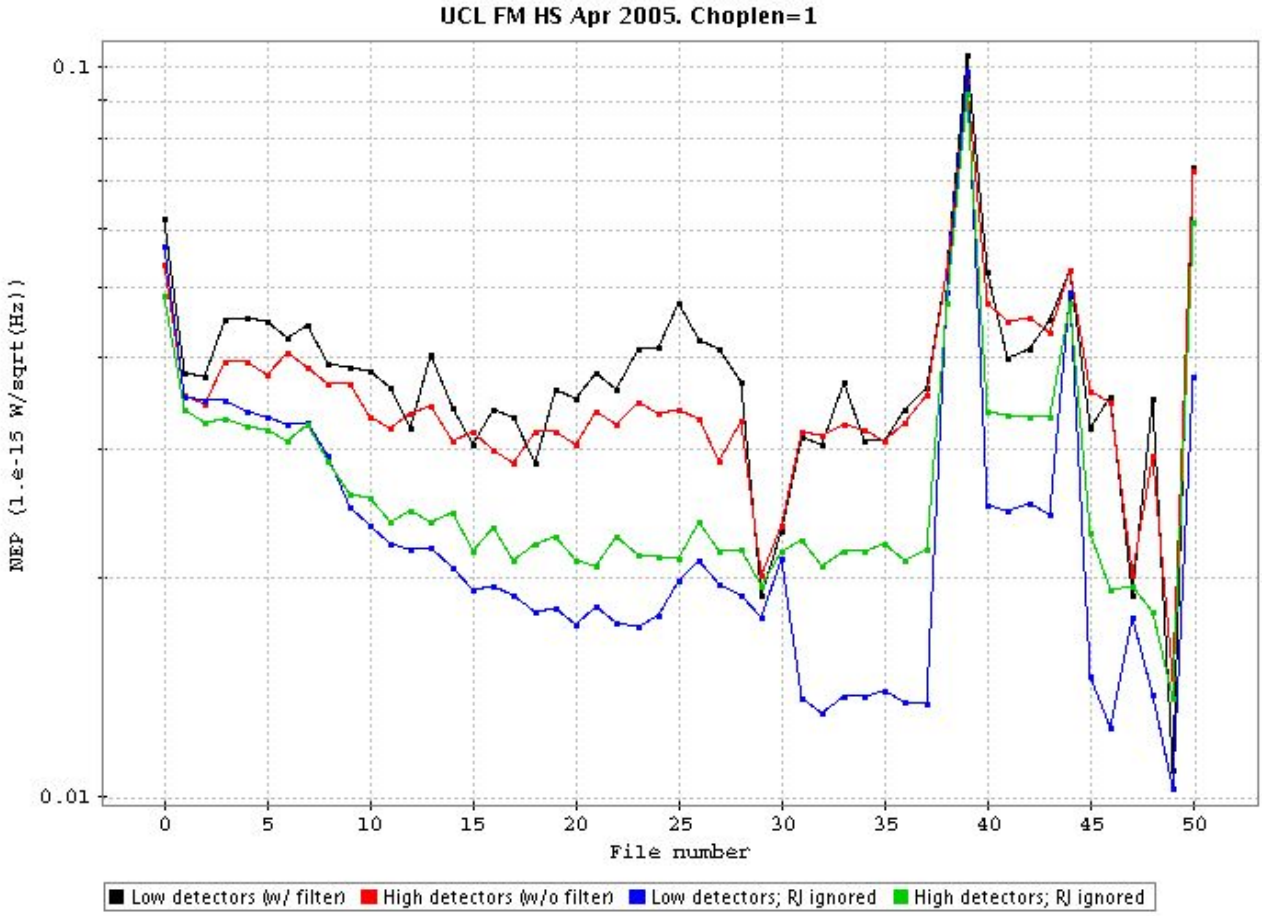

Figure 6 : Evolution of NEP with time for the FM HS data (described in RD05). Behaviour of low & high detectors (covered / not covered by the FIR filter) is compared for a chopper plateau of 1 ramp.The Cf & ramp length were 1.1pF & 0.25 second. The bias was 50mV up to file 30, 30mV from there to file 38, changing for each file after.

In order to remind the reader of the content of these data:

- files 1 & 2 are pre-beam references (file 0 is abnormally noisy)
- files 3 to 28 correspond to a continuous exposition to radiation => responsivity increase
- files 29 & 30 are again pre-beam references, corresponding to another detector setting
- files 31 to 37 are 'worst case' high responsivity plateau, in the same detector setting as files 29 & 30
- the remaining files correspond to various detector settings, (files 38, 39, 44, 47 & 49 are pre-beam references corresponding to these settings)

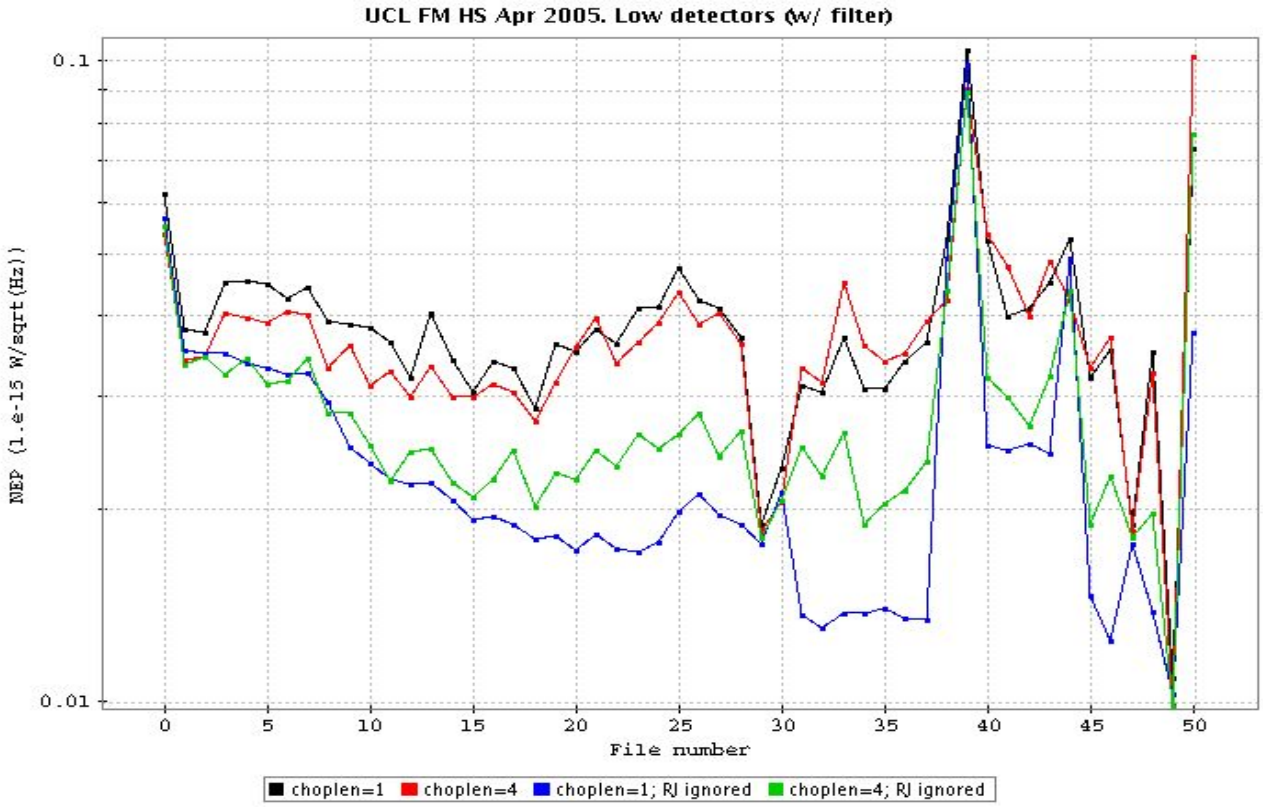

Figure 7 : Evolution of NEP with time for the FM HS data. Chopper plateaus of 1 & 4 ramps are compared for the low detectors (covered by the FIR filter)

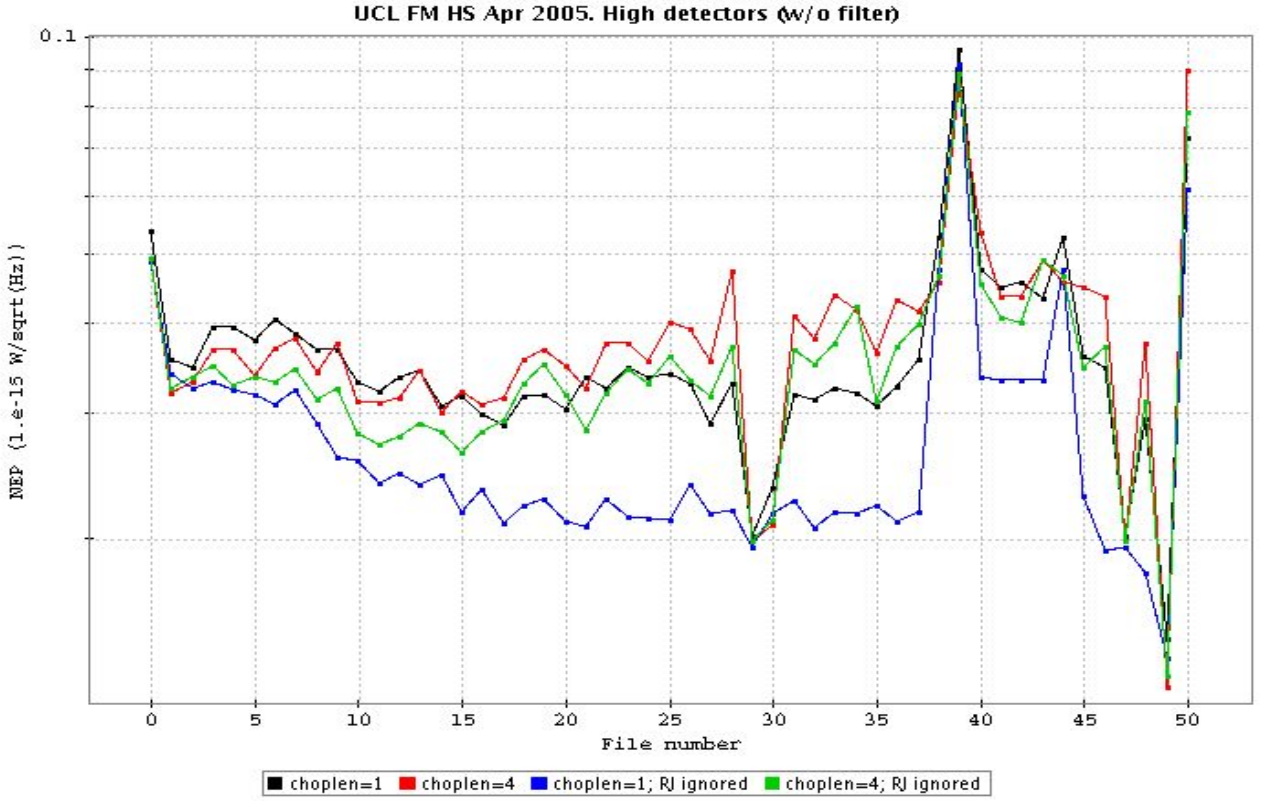

Figure 8 : As figure 7, for the high detectors (not covered by FIR filter). The y-range is the same.

This time, the **conclusions** are somewhat different :

- the data obtained under proton irradiation, with higher and higher responsivity seem less and less noisy. See note below for discussion of this
- the length of the chopper plateau has much less influence than it had on the QM data.
- the rejection of RJ is still efficient for choplen = 1 and less / not efficient otherwise.

- - - Note on the decrease of the NEP- - -

The NEP decrease in time is –a priori-- unexptected. The expected behaviour is the one observed for the QM modules. The first thing coming to mind is that there is an additional source of noise in the devices, dominating the photon noise, so that when the responsivity increases, the signal increases faster than the noise, hence showing a decrease of the NEP. What are the differences between the QM & FM tests ?

1. The CRE generation, QM -> FM. This **cannot** be responsible for the observed behaviour, as the FM modules are less noisy than the QM (from 6-Pack test analysis).
2. The bias. The QM test shown above was performed at 70mV, whereas the FM test was performed partly at 50, partly at 30mV. Looking at figure 8B, we see that the NEP is decreasing from low biases up to 70mV, after which it is increasing again, rather fast. On top of that, irradiatiing a Ge:Ga detector has a very similar effect as to increase the bias, namely an increase of responsivity. Hence, operating with a bias of 70mV during irradiation brings the detector in the fast rising part of the NEP vs bias curves, inducing an increase of the NEP. On the countrary, when operating the device at 30 or 50mV like during the FM test campain, the increase of responsivity will bring the system towards quiter zones, less noisy regimes, hence explaining figures 5 & 6...

Whether or not the measurements are dominated by an electonic source of noise rather than by photon noise remains matter of debate. although the dependance of the NEP on the integrating capacitance seems to give an indication in this direction.

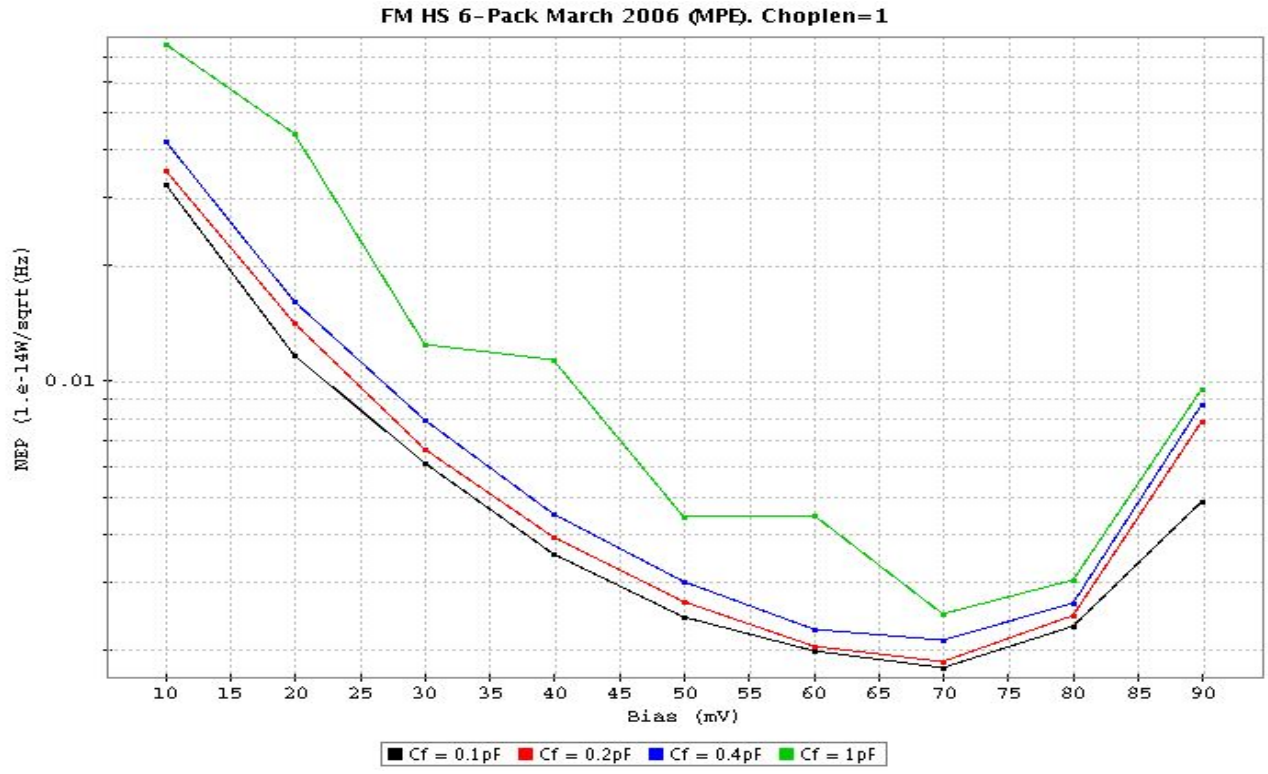

Figure 8B : NEP vs bias for the 4 possible integration capacitances. The device is a 6-Pack set of FM HS modules.

5.3 Third test run : FM LS

101 data files of the second test day were selected for analysis (the proton flux on the 1st test day was too high and badly calibrated). The exact list of files can be found in Table 1.

- files 0 to 4 are pre-beam references for files 5 to 33, 38, 41, 44 to 56, 59 & 100.
- files 5 to are 16 correspond to increasing responsivity
- files 17 to 22 were obtained with high proton flux, simulating solar flare, hence corresponding to extremely high responsivity (& noise)
- files 23 to 27 were obtained with low proton flux again, just letting the detector experience 'self curing' thanks to the FIR light applied.
- file 28 is a curing, via the flasher. It contains very sharp flux changes.
- files 29 to 56 correspond to a time range where the responsivity was increasing again after the curing. Files 41 & 44 to 56 we obtained with the same detector settings
- files 57 to 100 span a wide range of detector settings in terms of bias and ramp lengths
- files 67 & 68 are pre-beam references for file 71, and file 99 for file 96

The flux assumption adopted for the NEP computations were (RD03):

- “low detectors” (covered by the FIR filter) : 1.3 e-14W/pix
- “high detectors” (not covered by the FIR filter) : 1.8 e-14W/pix

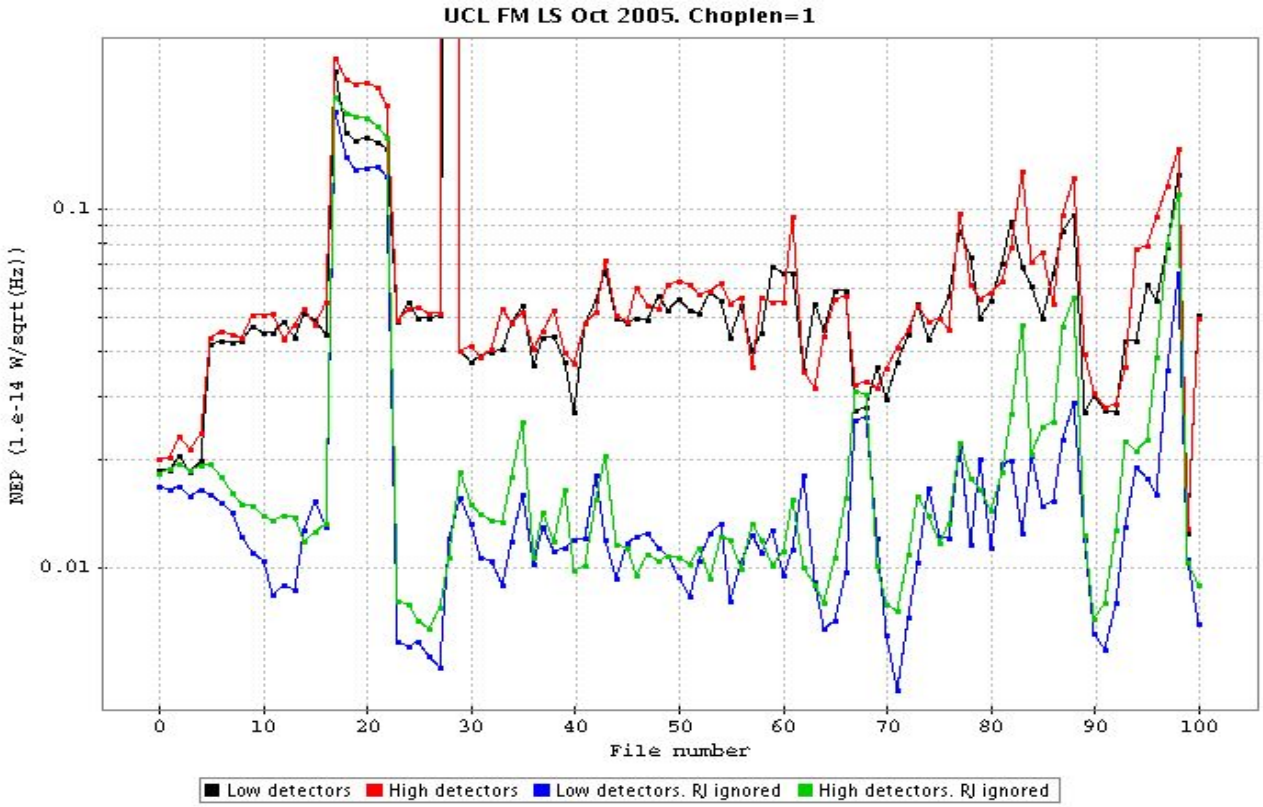

Figure 9. Evolution of NEP for the unstressed detectors. One ramp/ chopper plateau for all curves.

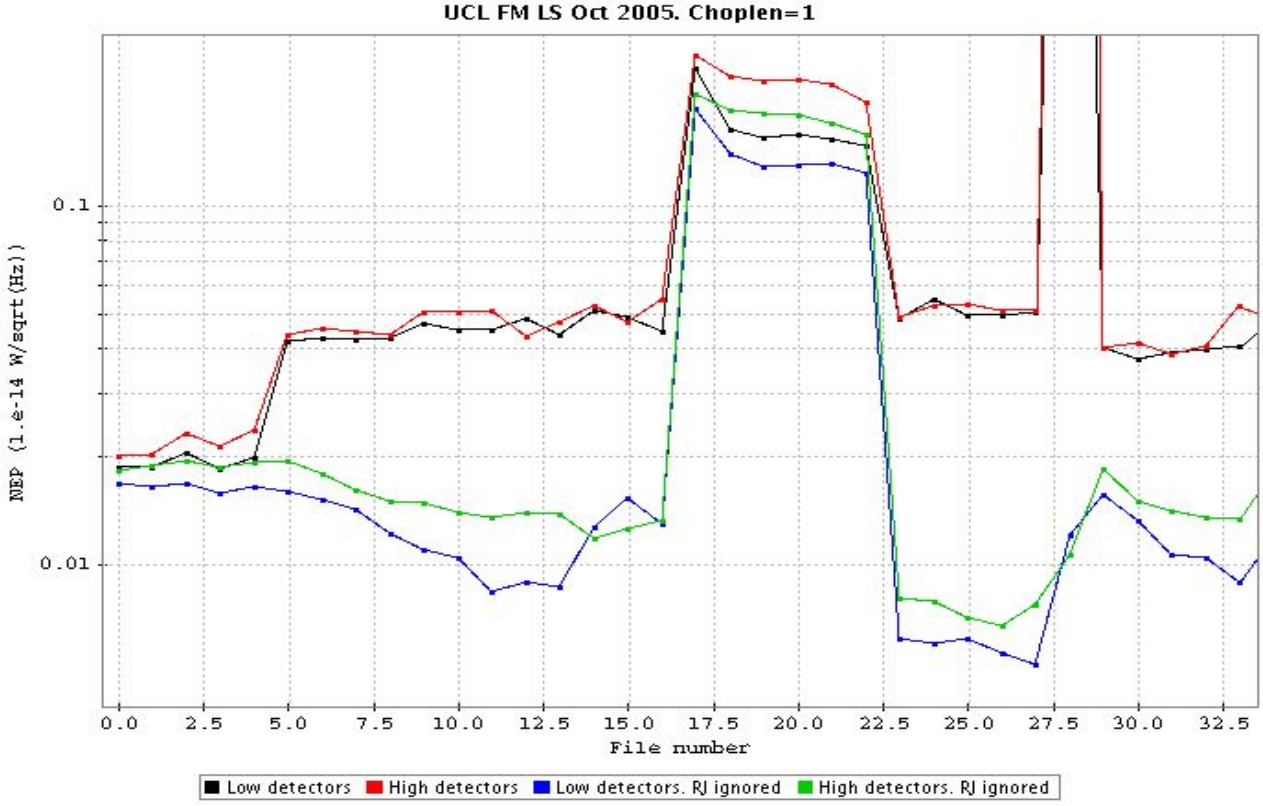

Figure 10. zoom on the starting sequence of figure 9 : pre-beam (0-4), low proton flux (5-16), high proton flux (17-22), low proton flux (23-27), flasher curing (28), low proton flux (29-33).

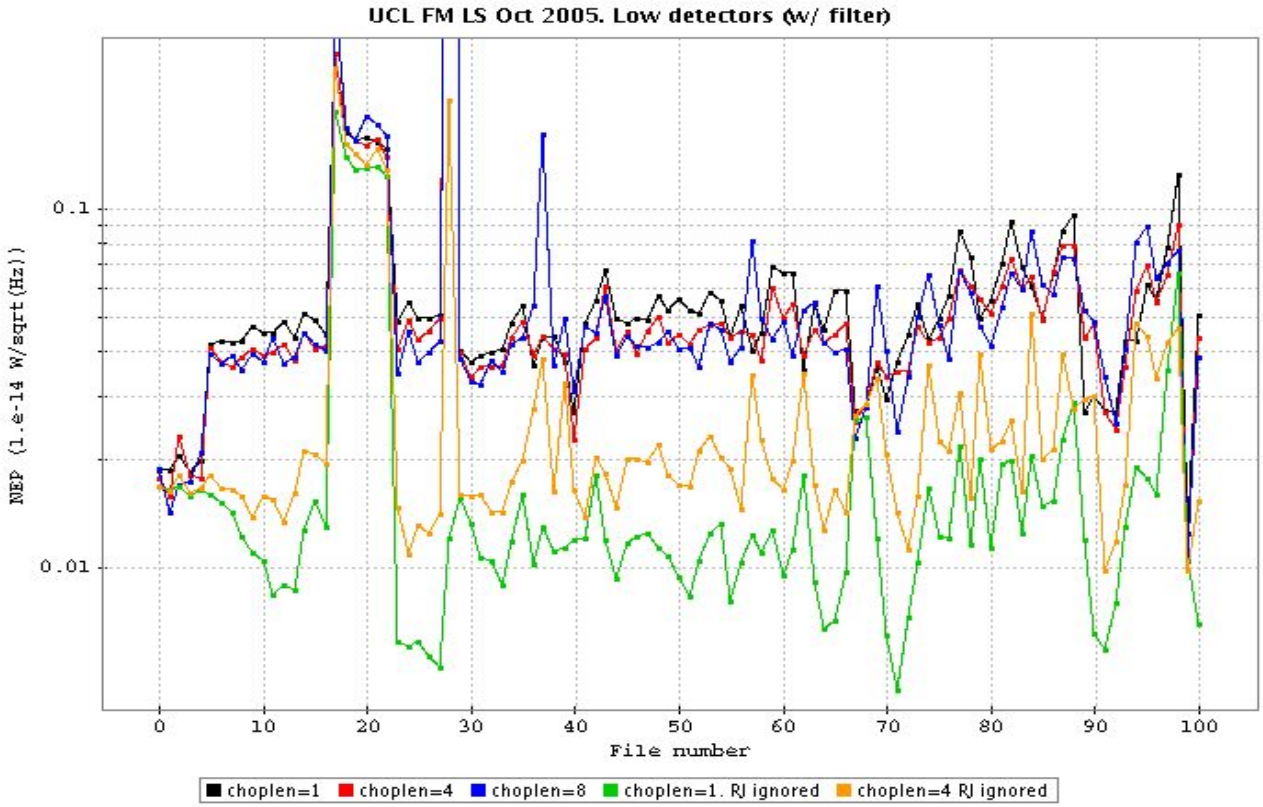

Figure 11 : evolution of the NEP for the unstressed detectors (covered by the FIR filter).

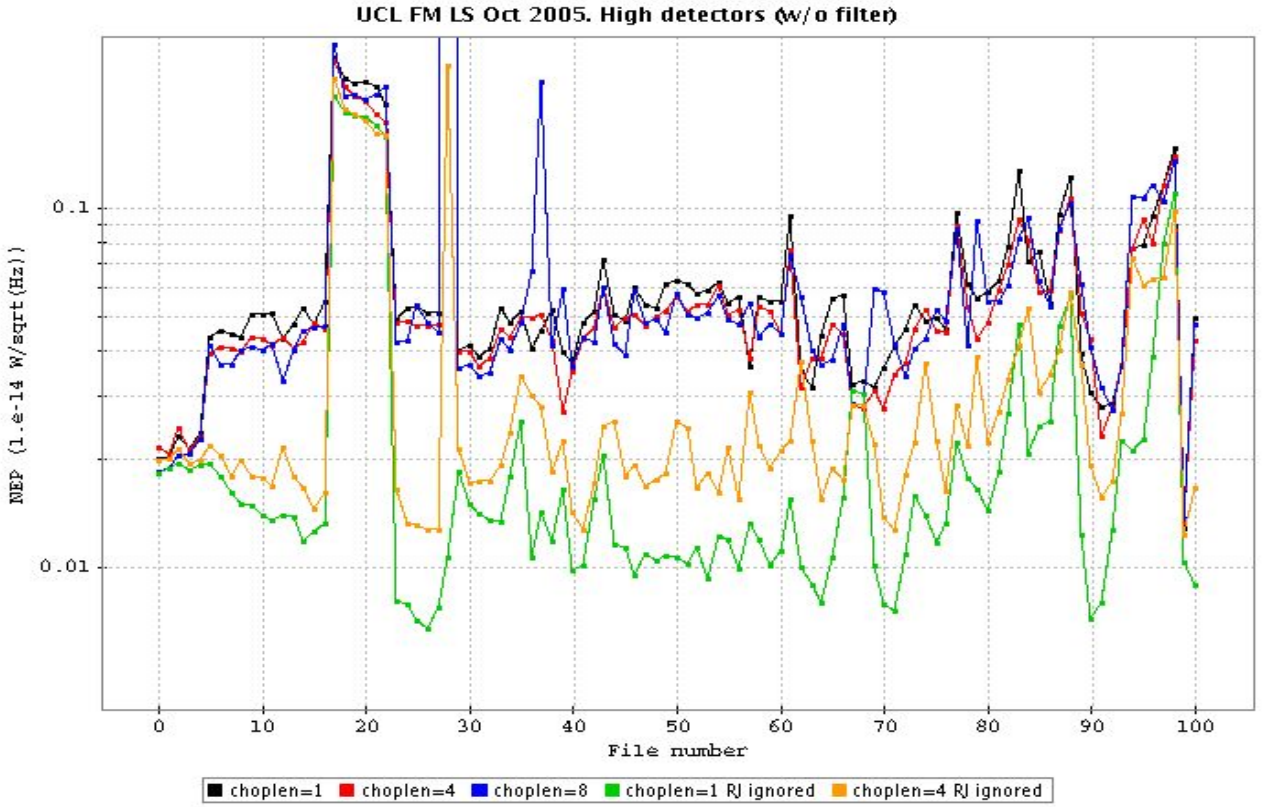

Figure 12. Same as figure 10, for the high detector numbers. The y-range is the same as in figure 11.

Figures 9 to 12 show some results. The main **conclusions** are that

- As for the second test run, and countrary to the first, the high responsivity data, supposedly severely affected by radiation effects, appear less noisy than pre-beam data once the RJ are detected & ignored.
- Again, countrary to the first test run, and consistently with the second, the length of the chopper plateau seems to have barely any effect on the final noise
- Here, the long term effects of the glitches on the responsivity are more subtle for the LS detectors. Indeed, the RJ correspond more directly to the effect of glitches on the slopes and, as such, are more isolated events. Hence, the detection/deletion of RJ keeps much more efficient than for HS data, even for longer chopper plateaus, whichever type of detector is considered (covered or not by the FIR filter).
- the pre-beam data are barely not affected by the rejection of RJ. This was of course to be expected.

5.4 Ideal Ramp Length

Data files 57 to 98 of the 3rd test run, on the LS module, were specifically obtained with the purpose to determine the best detector setting, in particular the best ramp length.

In the light of the conclusions of 5.2 & 5.3, it is unclear whether or not photon noise dominates the observed noise behaviour. One could nevertheless look at things this way : the data files we are dealing with here were all obtained under similar conditions, namely in the high responsivity plateau after a long exposition to proton radiation. Only the detector parameters were varied (ramp length & bias). So, if the hypothesis formulated above about an additional source of noise from the test setup is correct, and one still sees some clear differences between the various detector settings, that can only mean that these differences are sufficiently important to overcome the noise, hence, can be seen as significant...

Figures 13 & 14 show close-ups on the “RJ cleaned” chopped NEP for 1 & 4 ramps per chopper plateau, for both sets of detectors. As said earlier, the data with 1 ramp / chopper plateau are probably more relevant to investigate about differences between detector settings, but we want to check whether or not the conclusions we might draw from 1 ramp / chopper plateau remain at all valid for longer plateaus.

In Figures 13 & 14, the peaks of low NEP are located on files 64, 71 and 90-91. Except file 90, all the others correspond to a ramp length of ¼ second. Looking at figure 13 in a systematic way, (each set of files listed here below contains data for ramps of 1, ½, ¼, 1/8, 1/16 seconds, in this order) :

- files 89 to 93 : **bias = 60mV** : ½ & ¼ second perform equally well
- files 69 to 73 : **bias = 80mV** : ¼ second is clearly the best choice
- files 62 to 66 : **bias = 100mV** : ¼ second is clearly the best choise
- files 57 to 61 : **bias = 120mV** : ¼ &1/8 second perform equally well
- files 74 to 78 : **bias = 140mV** : ½ & ¼ second perform equally well
- files 79 to 83 : **bias = 160mV** : situation unclear, although ½ second would look like the best choice
- files 84 to 88 : **bias = 180mV** : ½ & ¼ second perform equally well
- files 94 to 98 : **bias = 200mV** : ½ & ¼ second perform equally well

One can argue that files 67 & 68, the pre-beam counterparts of file 71, exhibit a much higher NEP than file 71 itself while on the countrary, file 99, the pre-beam counterpart of file 96, exhibits a lower NEP than file 96... we can't answer that objection.

For the rest, ramps of ¼ second are among the best choices whatever the bias, whereas their best competitors, i.e. ramps of ½ second, being longer, offer more sensitivity to glitches and less flexibiliy in AOT design (wrt repetition of small buiding blocks, minimum duration of grating scans etc). If the data were finally declared suited for this investigation, we would hence recommand ramps of ¼ second.

In addition, it is interesting to see in figure 13 that the 3 best defined “valleys” of NEP, idenfified already at files 64, 71 & 90-91 all correspond to low detector bias : 60, 80 & 100mV. Even more, from 60mV to 120mV, NEP valleys of increasing bias appear shallower and shallower (local minima at files 91, 71, 64 & 59/60), and, for bias > 120mV, one cannot really speak of a 'valley' shape anymore! Hence, in case the detectors would never be cured, we would recommand to operate the unstressed detectors with a bias as low as 80mV, but of course, there is a trade-off between the optimum bias and the curing frequency: whereas 80mV seem optimal if we never cure, a higher bias might be optimal if we cure the detectors well before they reach this worst case plateau.

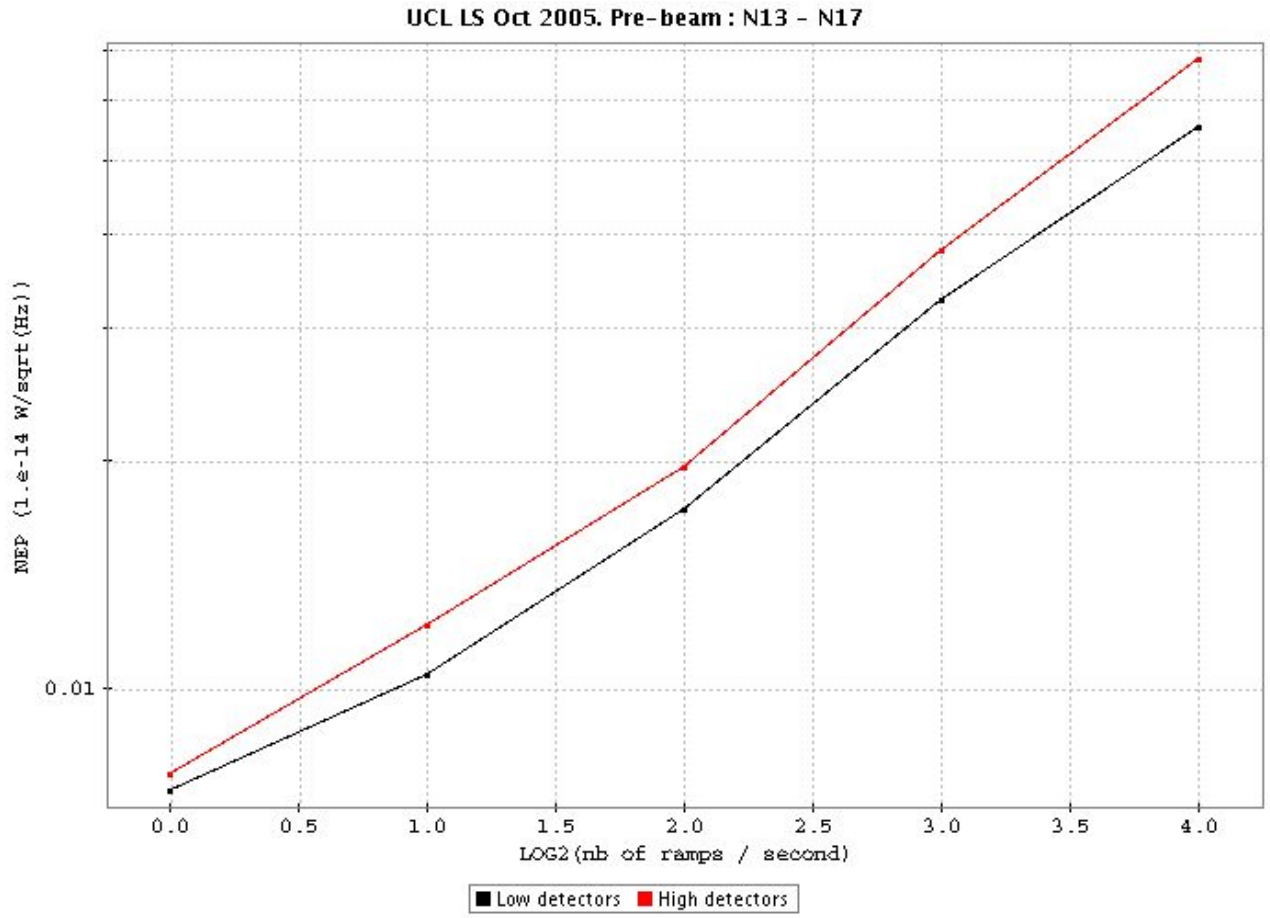

Figure 13A. NEP vs ramp length. Pre-beam data (Cf = 1.4pF, bias = 120mV).

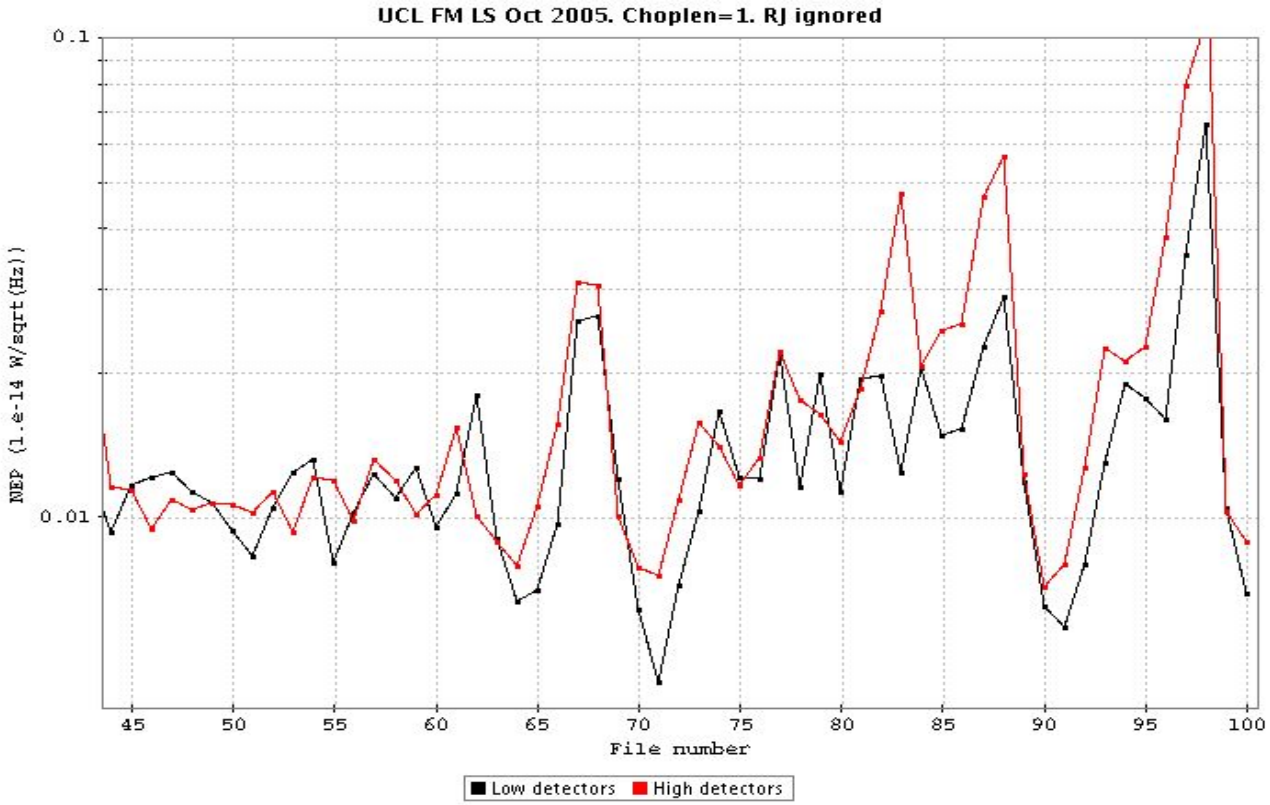

Figure 13 : NEP for various detectors settings (see text)., under low proton flux, at the high responsivity plateau. Simulated chopping with 1ramp per chopper plateau.

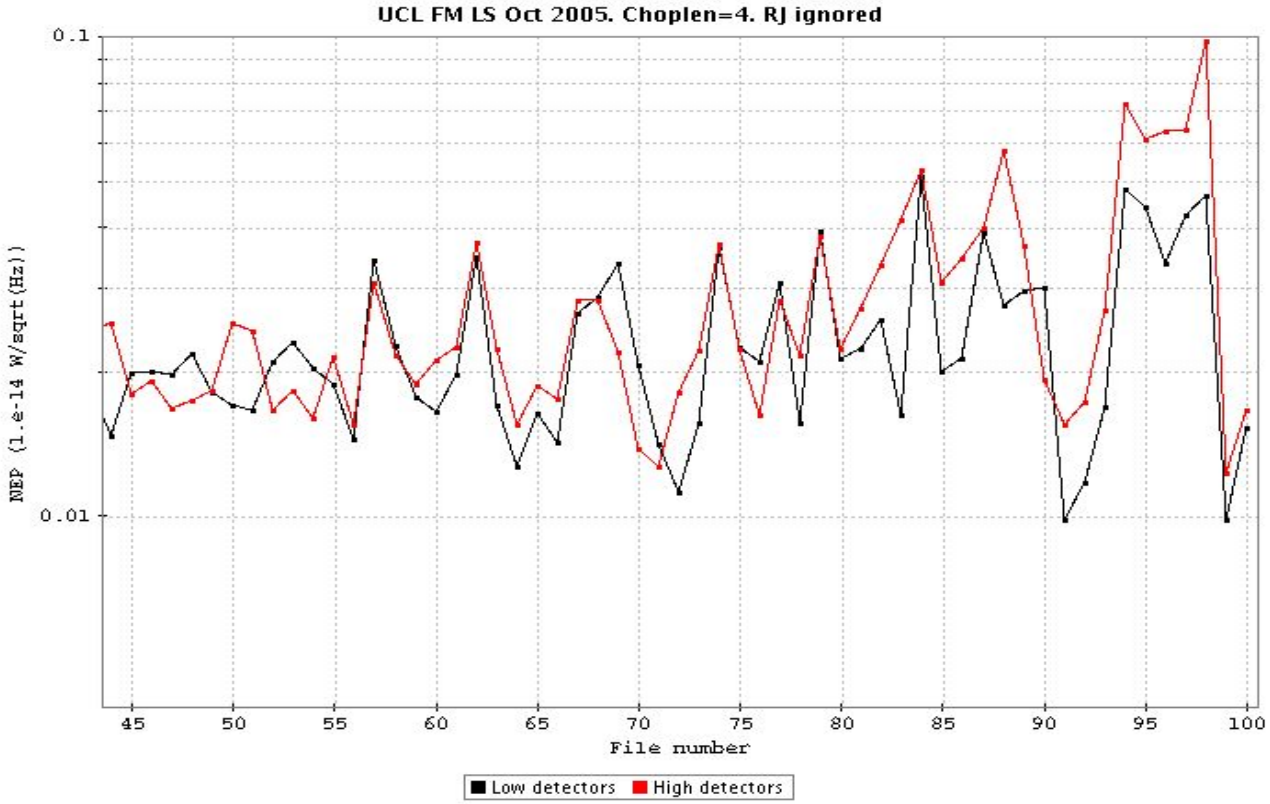

Figure 14 : as figure 13, with 4 ramps per chopper plateau.

6.Curing Frequency

Another critical parameter to assess for an efficient mission planning is the necessity/frequency of detector curings. This is expected to be a trade-off between various parameters. Amongst others:

- *the noise one can afford* : the longer the observations without curing, the more noisy they should become, unless we are dominated by an unexpected source of noise, as shown above. If we can afford never to perform detector curing, we will reach a plateau where the situation is stable, but with high responsivity, and also high noise (see RD06).
- *the number of "spiking" / useless detectors one can live with* : the higher the responsivity, the more detectors (should) start to exhibit a spiking behaviour (see figure 15).
- *the detector bias* : which directly impacts the detector responsivity. Hence, the higher the bias, the sooner the detectors enter in 'spiking mode'.

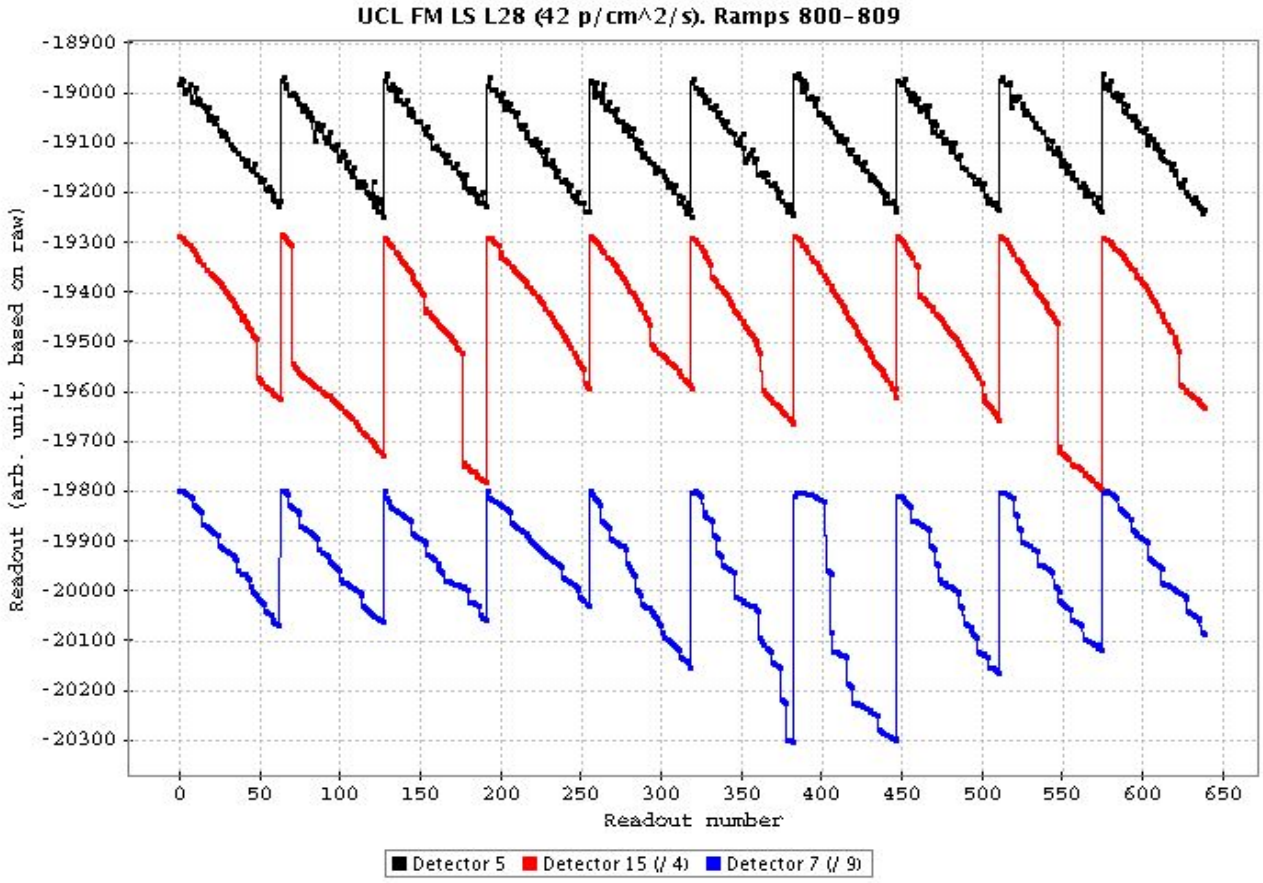

Figure 15 : 10 ramps, obtained simultaneously for 3 different detectors of the LS module (datafile L28). While detector 5 doesn't exhibit anything special (1 glitch from time to time), detector 15 exhibits more than 1 glitch per ramp, and detector 7 exhibits really chaotic behaviour due to multiple 'breakthrough'.

Figure 15 shows that with the same irradiation history, the various detectors have very different behaviour, i.e. their sensitivity to radiation effects, and to spiking is very different.

Several questions have to be answered

1. in normal conditions, i.e. outside of a solar maximum, should we expect detectors to spike if we do not cure them ?
2. by extension : for any given detector, how does the apparition of spiking depend on the detector

settings ?

3. during the PV phase where we want to fix the curint frequency, how can we automatically, from the ground, determine when a detector is spiking ?

We may try to answer the **first question** in an “empirical” way. For this, we simply look at the behaviour of our detectors during the 'rest phase' after the simulation of a solar flare, i.e. before real detector curing, i.e. in the 'worst case plateau'. For example, file LS_L82 (slopes in black & grey around ramp number ~26000 in figure 1). Inspection of these ramps (not shown here) and slopes (figure 16) demonstrate that, even in this 'worst case', the detectors are not spiking : the glitch rate looks about the same for all detectors and the apparent noise as well (here: roughly, i.e. from visual inspection of ramps and slopes). Hence, we may conclude that, **at sufficiently low bias, we can expect not to have detector spiking, even a long time after the last curing**, even in the “recovery phase” after a solar flare.

Answering the second question is way more difficult, but we can get some hints from the data. Figure 16 shows all slopes from all detectors for 3 files : LS_H5 (120mV), at the highest point of the solar flare simulation, LS_82 , discussed hereabove (120mV, post solar flare) and LS_L28, obtained right after a detector curing (via flasher, see figure 8 & 9 in RD06). While the high responsivity but low bias solar flare and post solar flare data show no detector spiking, the data obtained right after detector curing, but at higher bias exhibit some spiking detectors! Since all three files were obtained with the same integration capacitance (1.4pF), this clearly confirms that the **spiking behaviour depends critically on the bias**. Of course, the behaviour is **also very different from one detector to the next**, as can be seen from figures 15 & 16.

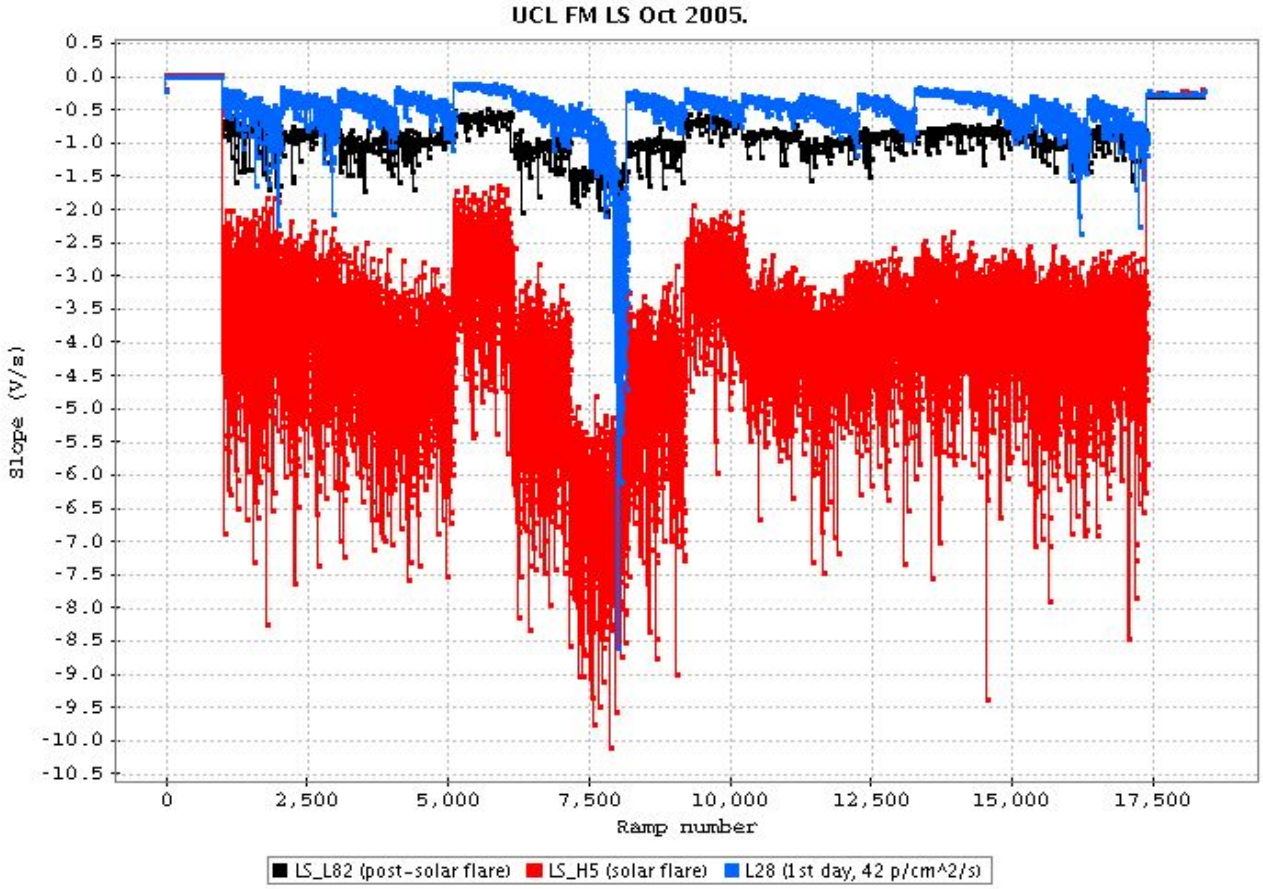

Figure 16: all slopes from all detectors for 3 LS data files : H5 (120mV, solar flare), L82 (120mV, post-solar flare) & L28 (200mV, post-curing). While the high responsivity but low bias solar flare and post solar flare data show no detector spiking, the data obtained right after detector curing, but at higher bias exhibit some spiking detectors.

Of course, a good answer to question 2 requires quantification, i.e. answer to question 3 : how can we automatically determine whether or not a detector is spiking ? This will of course be important in the PV phase, where we will most probably have to define or refine the curing procedure, and undoubtedly the curing frequency. Several options :

- glitch detection : if the glitch rate is very different among detectors, some must have a problem. Although overall glitch detection is not really an option on board, the raw ramps we will get from the downlink, rotating over the detectors, should be sufficient to determine a glitch rate for each detector over time.
- Responsivity : this is not an option : as shown on figure 16, the spiking / not spiking behaviour is independent from responsivity. On top of that, some spiking detectors have all their ramps very quickly saturated (e.g. detector 7 in file LS_150), hence mimicking a low responsivity...
- RJ detection : spiking detectors do not necessarily produce RJs, since the many “glitches” per ramp more or less level out from one ramp to the next. On top of that, the signal becomes so noisy that the number of detectable RJs actually drops when the detector starts to spike => not an option either.
- Noise : when the detector starts to spike, the slope of course becomes totally unstable. We will in any case have to define a noise level above which we decide that the detector signal becomes useless, so this should eliminate the spiking detectors for free.

To investigate the two options (glitch rate & noise), we need a data set where some non spiking detectors “turn on spiking”. For this, we use a bias sequence, made of data obtained for C=1.4pF, 256 ramps of ¼ second, bias sequetially increasing from 60 to 200mV (files L145, L125, L120, L115, L130, L135, L140, L150 in this order). Figure 17 clearly shows that the behaviour of detector 7 is becoming suspicious first, then completely erratic from bias=160mV on.|

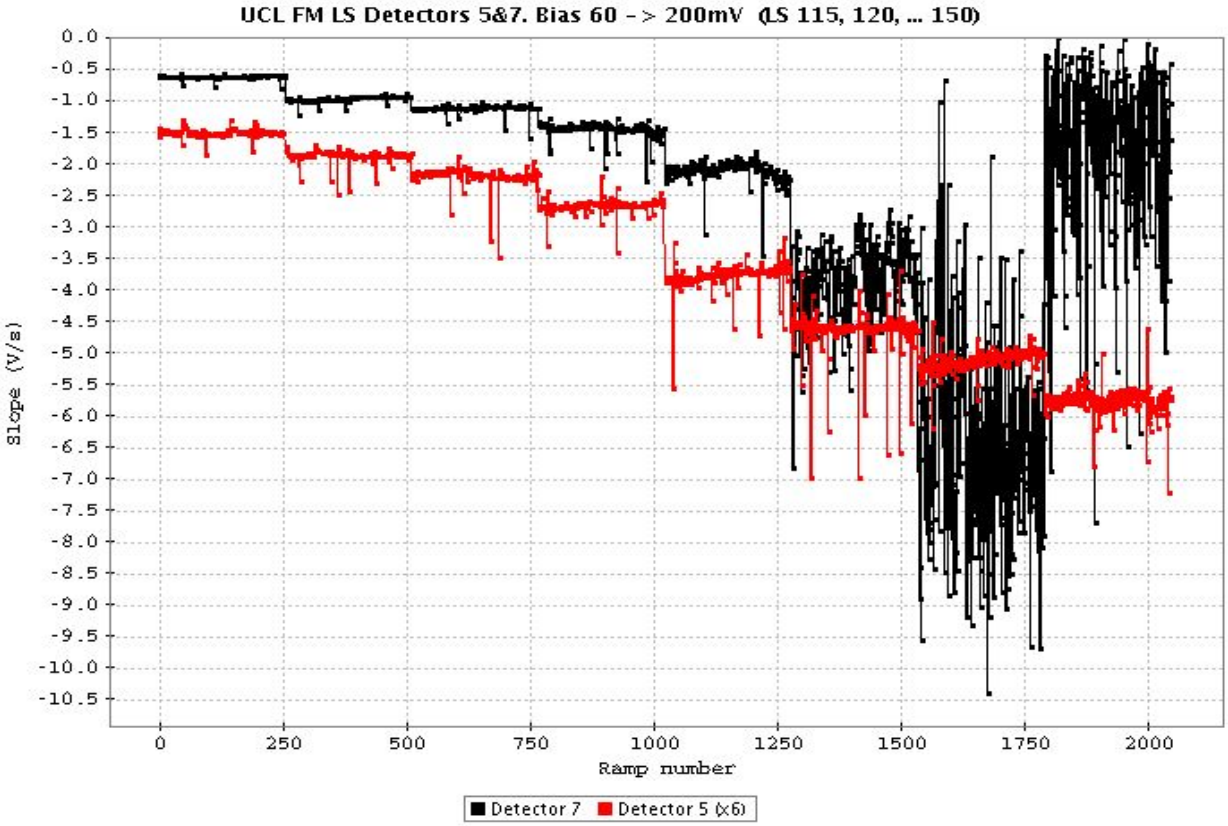

Figure 17. Bias sequence for ramps of ¼ sec. At bias 180 & 200mV, detector 7 is heavily spiking.

1. Glitch rate.

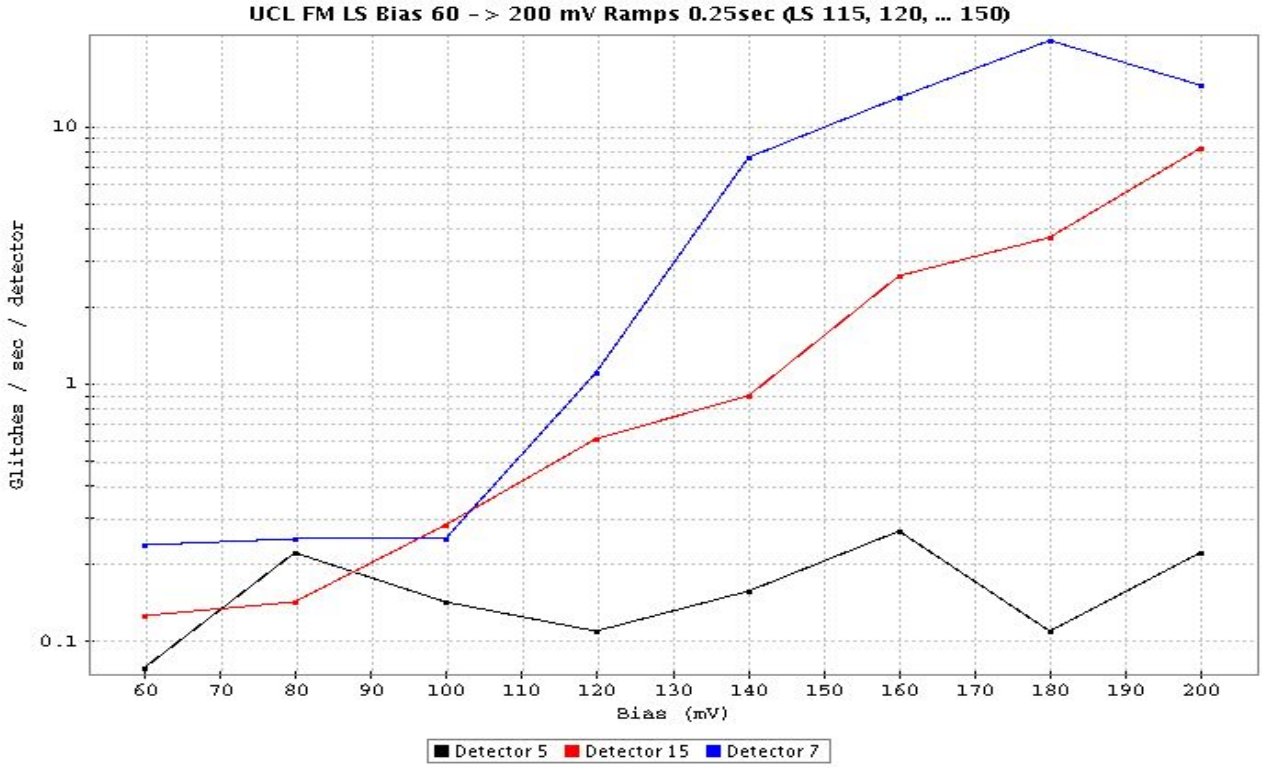

Figure 18. Glitch rate vs bias for 3 detectors. Whereas detector 5 shows a stable behaviour, the others show glitchrates growing exponentially with the bias. At 200mV, the ramps of detector 7 count so many glitches and are so quickly saturated that the glitch detection algorithm cannot work properly anymore.

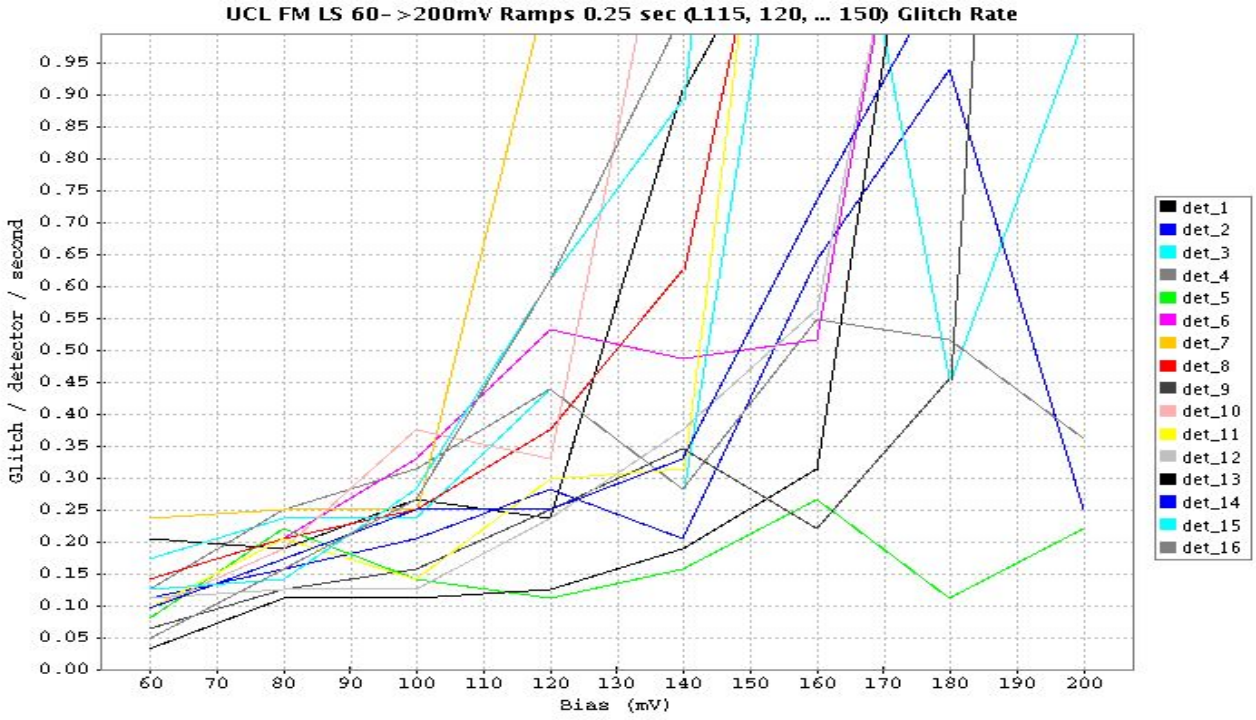

Figure 19. As figure 18, for all detectors, showing that the most sensitive ones exhibit a kink in the glitchrate as soon as bias > 100mV. At 200mV, almost all detectors are spiking.

Figure 18 & 19 show the progression of the glitch rate as a function of bias for various detectors. In figure 18, detector 5, which is not spiking, even at the highest bias, shows exactly the expected behaviour, i.e. its glitch rate is about constant around the expected value for ~10p/cm^2/sec (0.15 glitches/detector/second). The two other detectors, which are spiking at the highest bias values, show an exponential increase of the glitch rate, confirming the spiking behaviour.

Figure 19 shows that, for **bias > 100 mV**, the glitch rate explodes for **some detectors**, i.e. they **start spiking!** For bias > 120 mV, this concerns most of the detectors.

2. **Noise** : from figure 17, it seems obvious that there should be a kink in the noise of a detector when it begins to spike. To confirm it, we repeat the chopping exercice shown above, but this time, we inspect the noise of a single detector at a time instead of the median over a set of detectors. Figure 19 shows that the noise of the spiking pixel increases exponentially at high bias, with a kink between 140 & 160 mV.

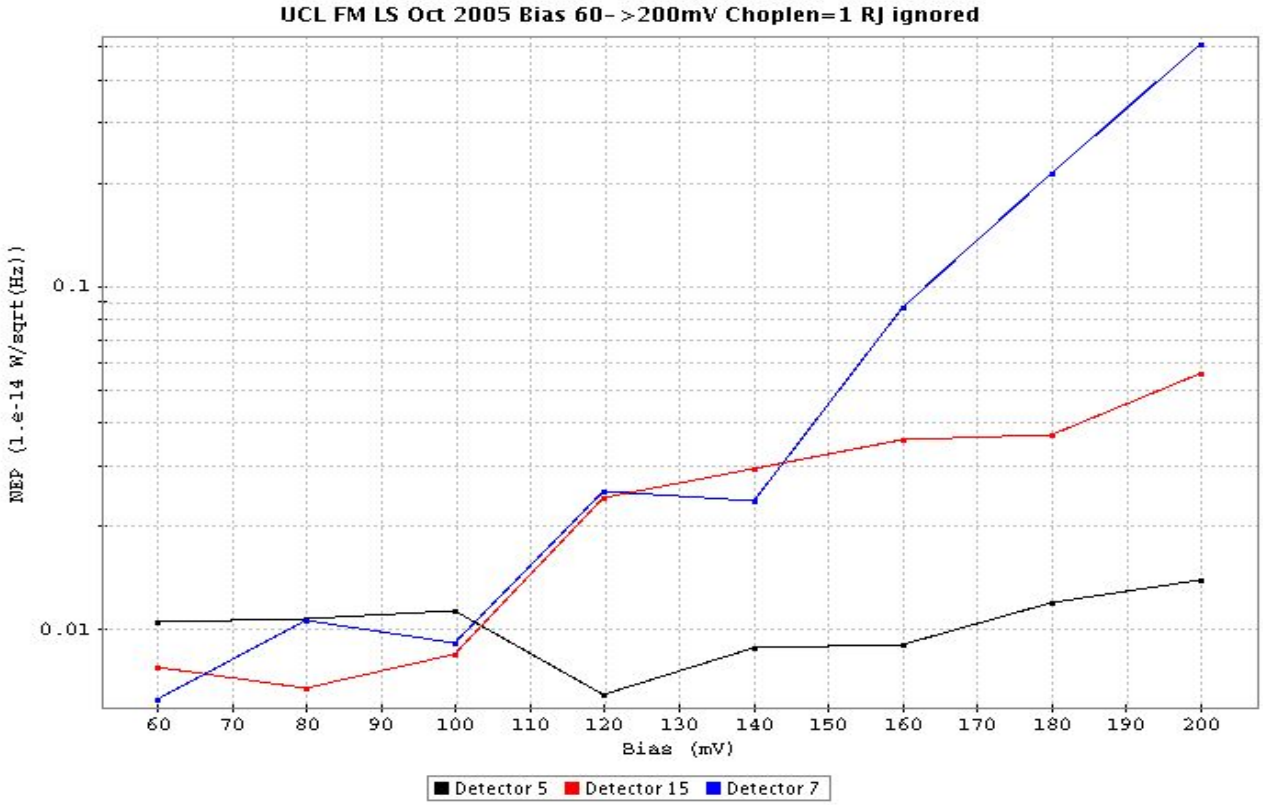

Figure 19 : NEP vs bias for 3 detectors. Detector 5 is stable, detector 15 & 7 show high noise for bias > 100mV

Summarizing, we confirm that, although the mathematical criterions are still to be defined, it should be easy to spot the spiking detectors from the huge glitch rates and noise they exhibit.

Undoubtedly, additional tests are required for HS & LS data in order to constrain the optimal bias & curing frequency. One can envisage to perform gamma irradiation tests on the ground, but, be it possible or not, it should be done or redone during the PV phase. At that moment, **we** simply **propose to obtain long stretches of data without curing for each of the various biases** between ~60 and 160 mV for the LS modules (~20 to 60 for the HS). Then, the best option for bias & curing frequency will be determined from the evolution of noise (i.e. also indirectly glitch rate or % of spiking detectors).

One might also think of taking a single long stretch of data, cycling through the various bias values. We nevertheless think that there are good reasons why this should be avoided :

- we need to investigate about the best curing frequency. This will be very different amongst the various bias values. Indeed, the responsivity, and noise, increase much faster at high bias than at low bias (e.g. compare figure 1 –bias=120mV-- and figure 6 –bias=200mV-- in RD06). Hence, it is to be expected that a higher bias will lead to a higher optimal curing frequency.
- the approach might be valid to investigate about evolution of glitch rate (i.e. % of spiking pixels) over time, provided we have enough raw data for each pixel. Assuming one can typically downlink 3 raw channels for each detector block (blue & red), rotating over the 400 pixels of the block at the rate of the SPU Buffers, i.e. every 2 seconds, and cycling over 6 bias values, we will return to the same pixel in the same configuration every 400 x 2 x 6 / 3 = 1600 seconds, neglecting overheads due to the bias modification. This is much too slow, since in the worst cases, it would mean we have only 2, 3 or 4 points per detector over the whole process from curing to high responsivity plateau. In this respect, gaining the factor 6 due to the iterations on the bias looks like a must.
- it cannot be excluded that, even in the lab, the behaviour of the detectors takes one or a a few minutes to stabilize after a bias change.

7.Conclusions

- Variations in the ramp length translate in significant variations in the NEP. Based on this, we would recommand ramps of **¼ second**.
- A method exists to flag the responsivity jumps in (unchopped) slope vs time signals*.
- The **chopper plateaus should be kept short**, i.e. 1 ramp, and if not feasable because of mechanism movements or other considerations, 2 ramps. Indeed,
  - **1.** short chopper plateaus means lower probability of a significant change of responsivity during (a consecutive pair of) plateaus. Hence, short chopper plateaus will end up in more well-behaved pairs of chopper plateaus with outlyers from time to time, whereas long chopper plateaus might lead to all chopper plateaus being affected by responsivity changes, i.e. translating to higher noise.
  - **2.** in the case of the HS modules, the longest the chopper plateau, the least effect the RJ deletion has on the final noise. Hence, if we aim at taking advantage of a RJ detection/deletion technique, we should keep chopper plateaus short.
- The spiking behaviour of the detectors depends critically on the bias. At sufficiently low bias (e.g. unstressed detectors at 100mV or less), no spiking behaviour appears even after a long period without curing or after a solar flare event.
- for NEP considerations, and to avoid spiking detectors, we recommand to use **low detector bias.** The optimum found from the NEP investigation on the unstressed detectors at their post-solar-flare-worst-case-high-responsivity was 80mV. Of course, there is a trade-off between the optimum bias and the curing frequency: whereas 80mV seem optimal if we never cure, a higher bias might be optimal if we cure the detectors well before they reach this worst case plateau.
- The **best curing frequency & detector bias** should be determined on basis of the “loss” of pixels because of their too high noise, or spiking behaviour. The exact mathematical criterions & values are still TBD, but a **“calibration” strategy** was **drafted for the PV phase** and possible additional gamma irradiation tests to be performed on the ground.

*The results of this operation might possibly be slightly improved by use of other methods (wavelets ? ... TBD).

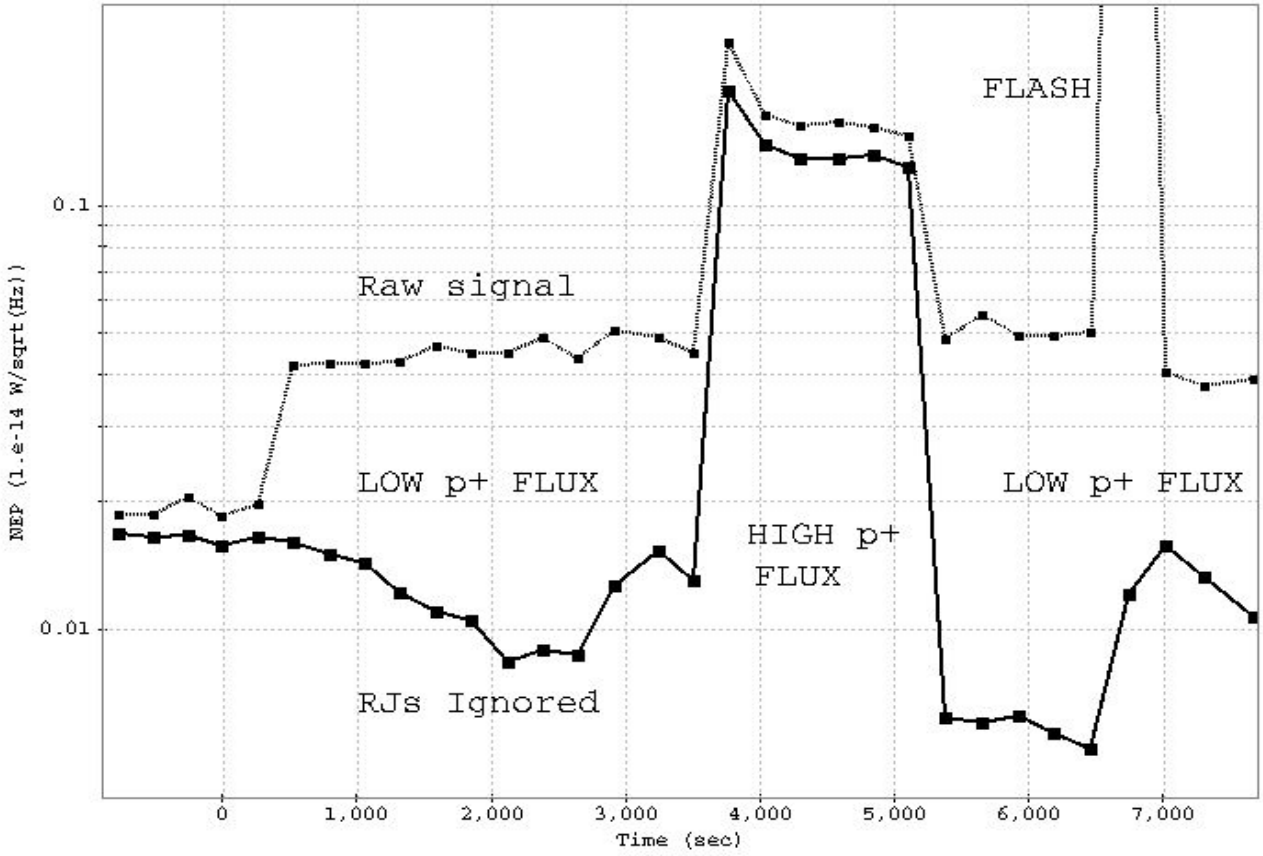
FLASH
Raw signal
LOW p+ FLUX
LOW p+ FLUX
HIGH p+ FLUX
RJs Ignored
0.1
0.01
NEP (1.e-14 W/sqrt(Hz))
0
1,000
2,000
3,000
4,000
5,000
6,000
7,000
Time (sec)

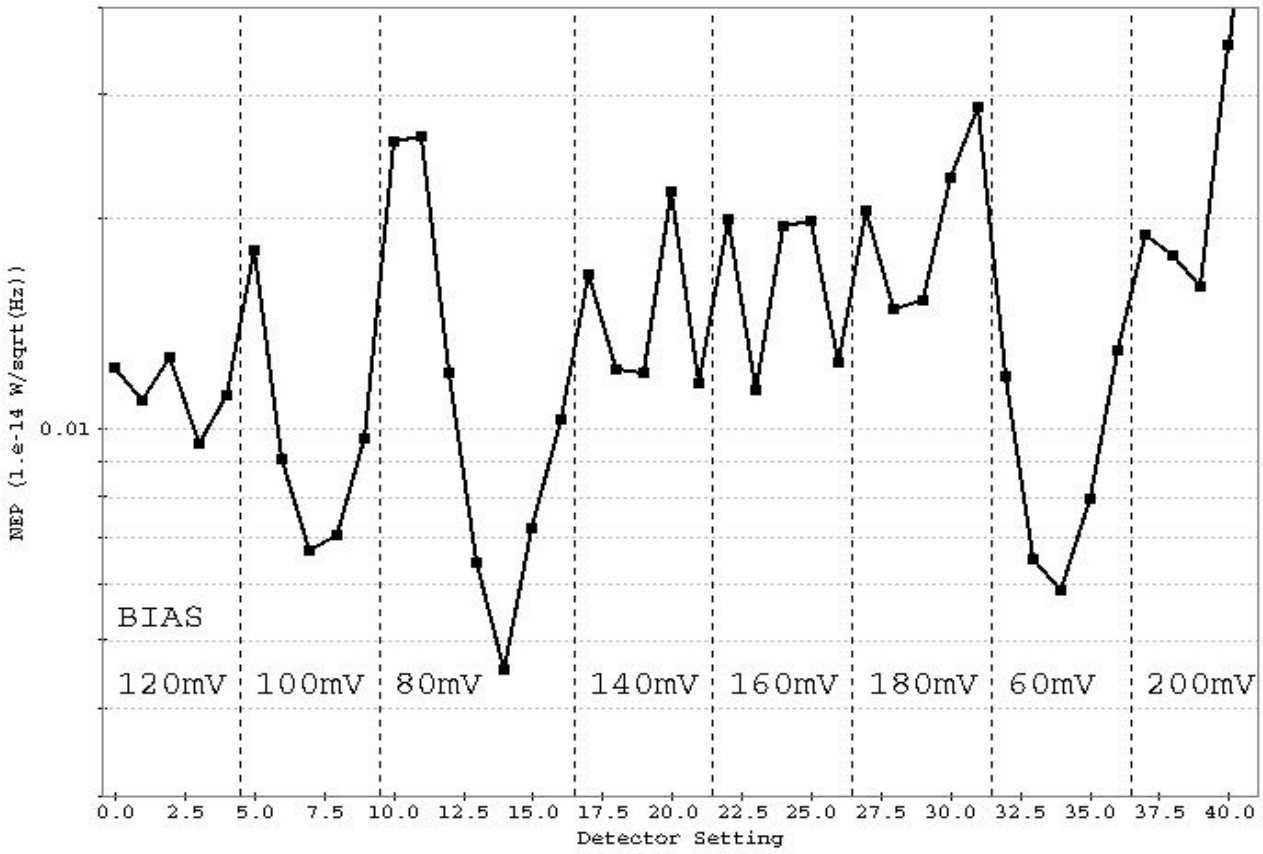
BIAS
120mV
100mV
80mV
140mV
160mV
180mV
60mV
200mV
0.01
NEP (1.e-14 W/sqrt(Hz))
0.0 2.5 5.0 7.5 10.0 12.5 15.0 17.5 20.0 22.5 25.0 27.5 30.0 32.5 35.0 37.5 40.0
Detector Setting

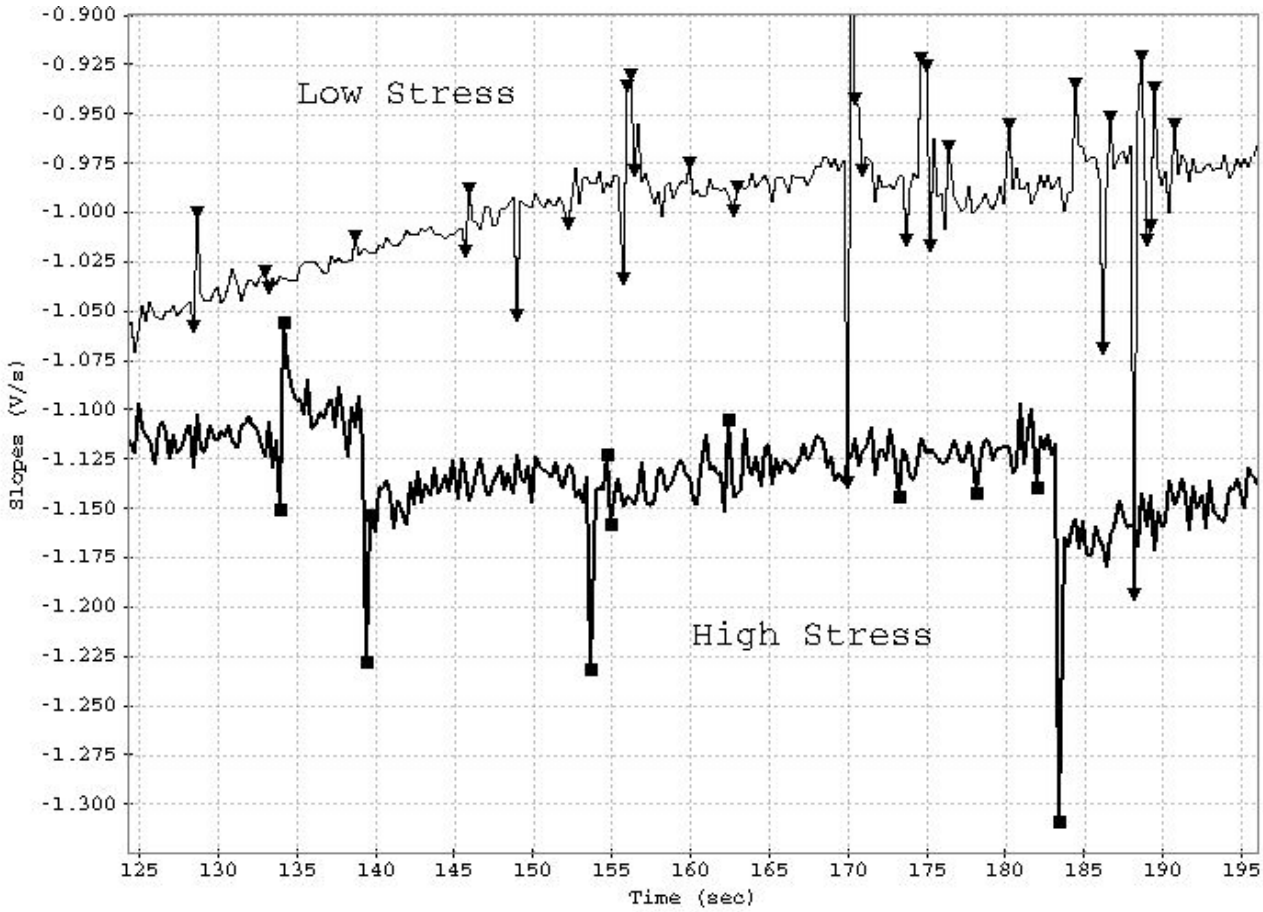
Low Stress
High Stress
Slopes (V/s)
Time (sec)
-0.900
-0.925
-0.950
-0.975
-1.000
-1.025
-1.050
-1.075
-1.100
-1.125
-1.150
-1.175
-1.200
-1.225
-1.250
-1.275
-1.300
125
130
135
140
145
150
155
160
165
170
175
180
185
190
195